MODELLING OF ALGAE TRAJECTORIES IN THE INTAKE CHANNEL OF SOUTH HUMBER BANK POWER STATION AND INTERACTION WITH BAND SCREEN FILTERS

BY

CHRISTOS NICOLAOU (ROB)

FOURTH YEAR UNDERGRADUATE PROJECT IN GROUP D, 2011/2012

I hereby declare that except where specifically indicated the work submitted herein is my own original work.

Signature: .... Date: ....

Contents

MODELLING OF ALGAE TRAJECTORIES IN THE INTAKE CHANNEL OF SOUTH HUMBER BANK POWER STATION AND INTERACTION WITH BAND SCREEN FILTERS
BY
CHRISTOS NICOLAOU
ROBINSON COLLEGE CAMBRIDGE UNIVERSITY

FOURTH YEAR UNDERGRADUATE PROJECT
IN GROUP D, 2011/2012

In this thesis a Lagrangian particle tracking method (LPTM) was used to develop a model for the trajectories of the algae plants in the intake filtering channel of South Humber Bank Power Station. The model was then used for implementing the interaction of the algae plants with the band screen filters. Open channel hydraulics equations were assumed to apply for the intake channel under investigation and suitable velocity profiles were calculated and imposed on the developed transport model. Suitable simulations for verifying the validity of the model developed were made.
The first part deals with the trajectories of the algae plants in the intake channel. Two different types of simulations based on the initial conditions were investigated, the instantaneous release of a large number of particles that are uniformly distributed along the depth of the channel and the continuous release of particles from the bed of the channel. For the instantaneous releases the model is tested for the case of a linear velocity profile along the depth of the channel and the results obtained were in agreement with other models using the LPTM approach. Then a logarithmic velocity profile in the smooth regime was imposed to the model and three different cases were studied. The first was for a constant diffusivity, the second was for a varying diffusivity, as given by Elders analytical result (1959), and the last case was an extension of the second case but now the buoyant forces on the particle were taken into account and thus a fall velocity was included in the numerical equations. For the continuous release the algae plants were released from the bed of the channel and their entrainment was studied. Concentration profiles were calculated for different water columns and the results obtained agree with similar numerical models of sediment entrainment concentration profiles. This verifies that the developed model describes the physical processes of entrainment well. The numerical equations were then extended to include a diffusive random step in the streamwise direction to represent turbulent diffusion. Simulations were made to compare the new results with the previous results. It was shown that the random diffusive step in the streamwise direction has a strong effect in the streamwise mixing of the algae plants in the near filed.
In the second part the developed model is used to implement the interaction of the algae plants with the band screen and suitable assumptions were made in order to model this. Simulations were made and based on appropriate defined parameters the number of algae plants blocked and passing through the screen were calculated. The results showed that

approximately 20 percent of the algae plants released accumulated on the bed before interacting with the band screen, the mesh panels of the band screen near the surface of the channel do not contribute to the screening process and also that the flexibility of the algae plants is an important parameter that affects the screening. Finally the differential level variation, across the band screen, with the percentage of the screen blocked was calculated. This showed that the differential level controls, which determine the cleaning process of the mesh panels, lie very close to eachother and are very sensitive to the percentage of the screen that is blocked. This gives rise to a potential triggering of the high differential alarm if the screen is not adequately cleaned after passing through the wash-water cleaning system.

Chapter 1

Introduction

1.1 Location

South Humber Bank Power Station (SHBPS) is located on South Marsh road near Stallingborough in North East Lincolnshire. It is a gas-fired combined cycle power plant with an output of 1266 MW. The station is operated and owned by Centrica SHB Ltd.

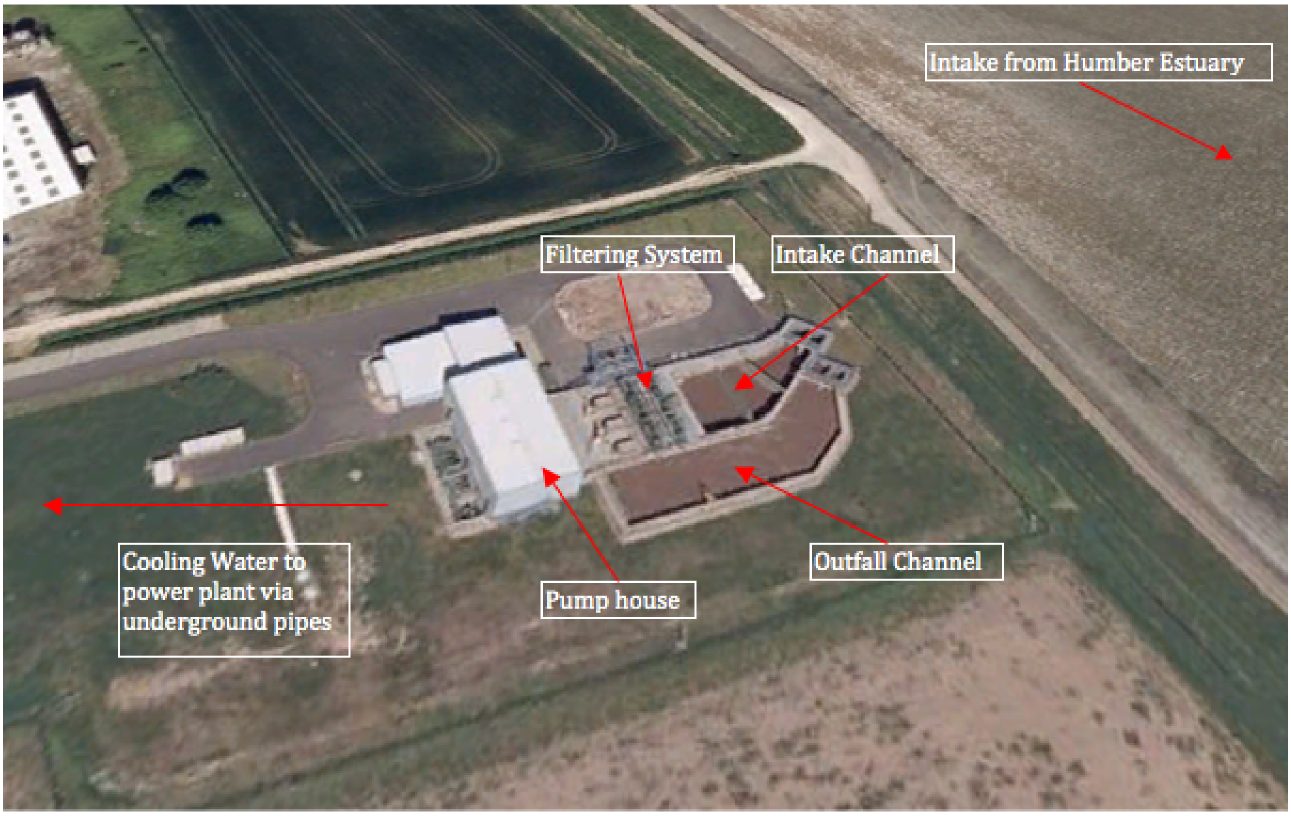

Figure 1.1: Intake System arrangement of SHBPS.

The station is made up of two phases. Phase one consists of three gas turbines and one steam turbine, while phase two consists of two gas turbines and one steam turbine. The station has a direct cooling system that draws water from the Humber Estuary using a submerged intake some 2 km offshore. The Cooling Water (CW) intake is a common system for both phases. There are three independent channels that each contains a coarse vertical rake, a fine vertical rake and a band screen. The latter is used for removing small particles which escape from the first two filters. Once past the three stages of filtration the water enters a suction fore bay from which the four CW Pumps (two per phase) draw the filtered estuarine water. The cooling water is then pumped to the power plant via underground pipes where it removes the waste heat from the main condenser and the closed cooling water inter-cooler. Figure 1.1 shows the arrangement of the intake system as it is on site.

1.2 Problem description

On two occasions, during March 2005 and December 2009, higher volumes of seaweed than normal were being brought in the intake filtering channel along with the estuarine water and the mechanical cleaning system of the band screens was not coping with this. The band screens were clogged from the seaweeds which resulted in a significant reduction of the flow rate through the screens. Because of the blockage of the flow, the level in the suction fore bay of the CW pumps dropped at the point where one of the CW pumps started to vibrate reaching the first alarm point. The CW pumps had to be shut down in order to avoid damaging them. Doing so requires shut down of the gas turbines. The band screens were damaged by the water pressure exerted on them and there was a failure of the gearbox bearing driving one of the screens. The mechanical system had to be turned off in order to repair the damages.

(a) Clean Band Screen.

(b) Blocked Band Screen.

Figure 1.2: Band Screens.

The problems developed through the system failure that occurred on the 30^{th} of December in 2009 were reported as follows: *(i)* The band screens level control indicated a high differential in levels. *(ii)* Band screens No. 1, 2 and 3 tripped due to seaweed overload. *(iii)* Band screens filtration panels were damaged and badly distorted by the pressure placed on them, allowing seaweed and other waste to enter the CW pumps suction fore bay and then the condenser water boxes [1].

Figure 1.3: Condenser water box with blocked tube bank.

1.3 Life cycle and morphology of red algae: Polysiphonia Lanosa

Red algae have numerous categories. One specific red algae named *Polysiphonia Lanosa*, is the algae identified for blocking the band screens at the intake filtration system of SHBPS.
It grows epiphytically on the brown seaweed *Ascophyllum Nodosum* and has a triphasic life-cycle, consisting of one haploid (male and female gametophytes) and two diploid (carposporophyte and tetrasporophyte) generations.

An individual plant of Polysiphonia Lanosa consists of a number of fronds growing out of a prostrate base with an extensive rhizoid system penetrating the host tissue. The main axis of the plant is strong whereas the branches are less strong and more flexible. Figure 1.4(a) shows a schematic of the pattern of the fronds. Reports and studies recorded a range of lengths for this specific algae depending on their age. Older plants were recorded to have a maximum length of up to 30 mm while younger plants have a length of around 8-10 mm. Plants of all ages were recorded to have a similar range and mean number

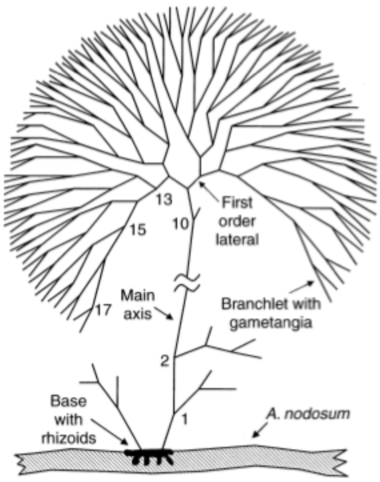

(a) Schematic representation of a frond of Polysiphonia Lanosa illustrating the pattern of ramification.

(b) Polysiphonia Lanosa plant on parent seaweed.

Figure 1.4: Polysiphonia Lanosa.

of branching levels. Polysiphonia Lanosa is photoautotrophic, meaning it uses light as an energy source to convert inorganic material into organic matter. For this reason it does not extend far into estuaries nor in large depths, as the low light conditions are not suitable for the growth of the algae. Therefore it is usually found in shallow waters and on rocky shores as well as in places where its parent seaweed grows [2].

1.4 Objectives

This project aims to provide a model for the trajectories and hence the positions of the algae plants in the intake filtering channel as well as model their interaction with the band screen filters. Suitable simulations will then provide information about the dynamic movement of the plants and also the effects of the blockage of the band screens. Finally conclusions about the model developed and the band screens, as well as recommendations to avoid problems similar to those described earlier, will be derived.

Chapter 2

Theory and Methodology

2.1 Theory

2.1.1 Computer simulation

At the beginning of the project different paths were considered as how to proceed. The choice was between a computer simulation and an experimental investigation of the problem. The first was chosen due to the high cost and complexity of a scaled model for an experimental implementation of the particular problem. By choosing to do a computer simulation there was a need to choose the appropriate tools. Various commercial packages exist for analysing flows for a specified geometry, but they are very expensive and are mostly used by professionals who are trained; such packages are used by consulting companies designing the particular systems. There was a need therefore to develop a code with tools usually used for modelling in university research. Thus a code was developed using MATLAB.

Different transport models and methods exist applicable for the description of the algae motion in the intake filtering channel. These include Eulerian, Lagrangian, mixed Eulerian-Lagrangian and TVD methods. The Eulerian transport models, use finite differences or finite elements methods, and are often plagued by numerical dispersion or artificial oscillations especially for advection dominated problems. To overcome these problems a higher grid resolution and smaller time steps are needed, doing so results in large computational effort with long execution times. The mixed Eulerian-Lagrangian model combines the advantages of Eulerian and Lagrangian methods in treating the advection term with a Lagrangian approach and the dispersion and other terms with an Eulerian approach, however this approach does not guarantee mass conservation and is computationally more demanding than the Lagrangian method. In the case of TVD methods, which are higher order finite difference methods, they can reduce numerical

dispersion and artificial oscillations and are also mass conserving, but such methods require high computational effort. Finally the Lagrangian approach offers computational efficiency even when simulating large numbers of particles, and because of the simplicity of the explicit equations it can be easily implanted over any type of flow model. Also due to the use of particles as discrete mass parcels, global mass conservation is automatically satisfied [3].
The model developed for the computer simulation of the algae plants should be able to calculate the trajectories of all the algae plants in the intake filtering channel, be able to simulate a large number of particles and also have low computational needs. Taking into account the above requirements the **Lagrangian method** is chosen to develop the model for the computer simulation.

2.1.2 Lagrangian Particle Tracking Method (LPTM)

By considering the Lagrangian approach the **random walk particle tracking** method is adopted. This particle tracking method was formed from the statistical mechanical transport theories of Taylor (1921) and is basically a Monte Carlo based simulation of the problem of 'random walks'(Kinzelbach 1988)[4].

The transport is governed by the advection-diffusion equation:

$$\frac{\partial c}{\partial t} + \nabla \cdot (\mathbf{u}c) - \nabla \cdot (\mathbf{D}\nabla c) = 0 \tag{2.1.1}$$

where $\mathbf{u}$ is the velocity vector, $\mathbf{D}$ is the diffusion tensor, c is the concentration and t is the time. It is possible to derive a form of a solution to the above equation by transforming the whole solution process into the solution of a Stochastic Differential Equation (SDE), also called the Langevin equation which is an ordinary differential equation containing a deterministic part and an additional random 'noise' term. Doing so equations describing the movement of a particle for a small timestep Δt are derived.
In the case when the advection-diffusion equation has constant coefficients the position of a particle can be described by:

$$\mathbf{x}_{t+\Delta t} = \mathbf{x}_t + u\Delta t + \xi\sqrt{2D\Delta t} \tag{2.1.2}$$

where $\boldsymbol{x}_t$ is the location at time t, u is the advective velocity, D is the diffusion coefficient and ξ is an independent normally distributed variable with zero mean and unit variance. For the case however when the velocity and the diffusion coefficient vary in space, the equation becomes:

$$\mathbf{x}_{t+\Delta t} = \mathbf{x}_t + u(\mathbf{x}(t))\Delta t + \xi\sqrt{2D(\mathbf{x}(t))\Delta t} \tag{2.1.3}$$

with the constraint that Δt is small enough so that the velocity and diffusion coefficients do not vary much between $\mathbf{x}_t$ and $\mathbf{x}_{t+\Delta t}$.

A problem with the above approach, when the velocity and the diffusion coefficient vary in space, is that mass tends to gather in areas of low diffusivity. Two different methods were suggested to overcome this problem by I$\hat{to}$ and Stratonovich.

I$\hat{to}$ proposed the following correction:

$$\mathbf{x}_{t+\Delta t} = \mathbf{x}_t + \left[u(\mathbf{x}) + \frac{dD}{dx}\right]_{\mathbf{x}=\mathbf{x}_t} \Delta t + \xi\sqrt{2D(\mathbf{x}(t))\Delta t} \tag{2.1.4}$$

whereas Stratonovich suggested:

$$\mathbf{x}_{t+\Delta t} = \mathbf{x}_t + \left[u(\mathbf{x}) + \frac{1}{2}\frac{dD}{dx}\right]_{\mathbf{x}=\mathbf{x}_{t+\Delta t/2}} \Delta t + \xi\sqrt{2D(\mathbf{x}(t+\Delta t/2))\Delta t} \tag{2.1.5}$$

Both methods adjust the advective velocity by a *noise induced drift component* that involves the derivative of the diffusion coefficient in space [5]. It has been shown that the effect of the noise induced drift component is for areas of low diffusivity to tend to repel the particles whereas areas with high diffusivity tend to attract them. Therefore providing the necessary correction to equation 2.1.3.

2.2 Model setup

2.2.1 Intake channel geometry

Water from the Humber Estuary is drawn into the intake filtering channel via a circular pipe at a rate of 99000 m^3/hr (27.5 m^3/sec). The intake filtering channel to be modelled is of rectangular shape. The model developed will consider the schematic of the intake channel shown by figure 2.1 for simulating the interaction of the algae plants with the band screen. The intake filtering channel is modelled as an open channel and therefore open channel hydraulics equations are applied. An important geometrical parameter in an open channel is the hydraulic radius which is defined as the ratio of the channel's cross-sectional area of the flow to its wetted perimeter (the portion of the cross-section's perimeter that is wet), and is given by: $R_h = A/P_{wet}$.

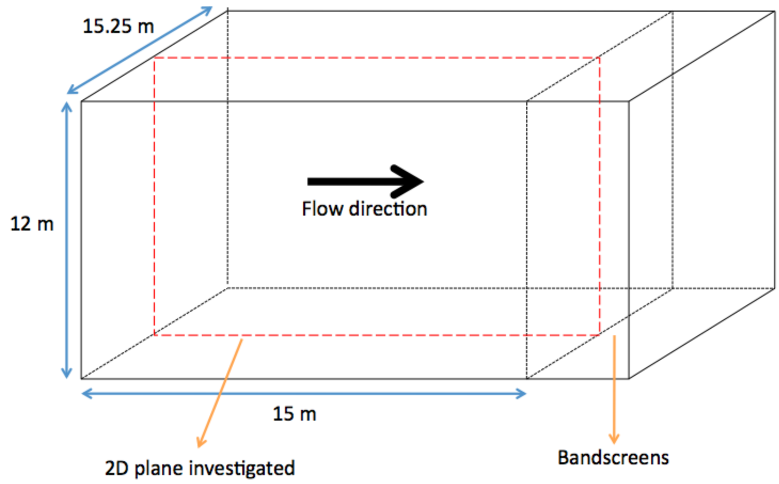

Figure 2.1: Schematic of intake filtering channel.

2.2.2 Velocity profiles

By knowing the intake volumetric flow rate and applying continuity between the intake pipe and the intake filtering channel the mean velocity in the intake channel is found to be $U = 0.150 m/sec$ (see A.1 Appendix A).
An assumption of the velocity profile in the intake channel is made by considering open channel hydraulics equations. Two different logarithmic velocity profiles which vary with the depth of the channel are used based on the type of the channel bed.

For a smooth bed the logarithmic velocity profile is said to be in the hydraulically smooth regime and is given by:

$$\bar{u}(y) = \frac{u_*}{k} \ln \left(9 \frac{y u_*}{\nu} \right) \tag{2.2.1}$$

whereas for a rough bed the corresponding equation for the velocity profile is:

$$\bar{u}(y) = \frac{u_*}{k} \ln \left(30 \frac{y}{k_s} \right) \tag{2.2.2}$$

and is said to be in the hydraulically rough regime. In the above equations u_* is the shear bed velocity, k is the von Karman constant (=0.4), k_s is the roughness height, y is the vertical distance from the bed of the channel and ν is the kinematic viscosity of water. The analysis for calculating the velocity profiles follows as well as relevant figures (figs. 2.2 and 2.3) showing the calculated velocity profiles.
The hydraulic radius of the intake channel is $R_h = 4.662\ m$ and the bed of the channel is made of concrete so the manning coefficient will be $n_{concrete} = 0.012$.

The shear velocity is calculated using the equation:

$$u_* = \sqrt{\frac{gn^2U^2}{R_h^{1/3}}}$$

and is found to be equal to $u_* = 4.36 \times 10^{-3}\ m/sec$. Hence using equations 2.2.1 and 2.2.2 the velocity profiles shown below are obtained.

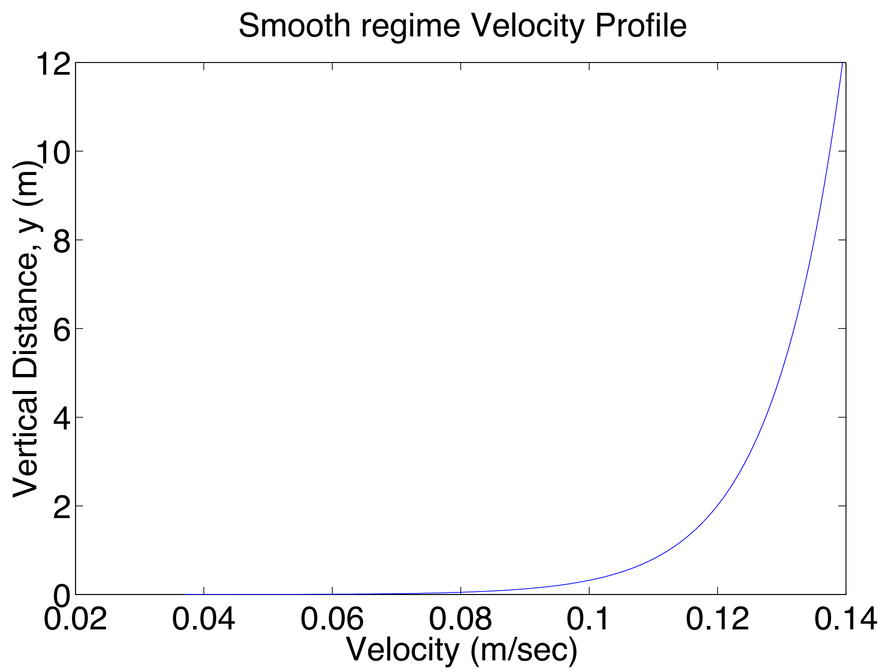

Figure 2.2: Smooth Regime Velocity Profile.

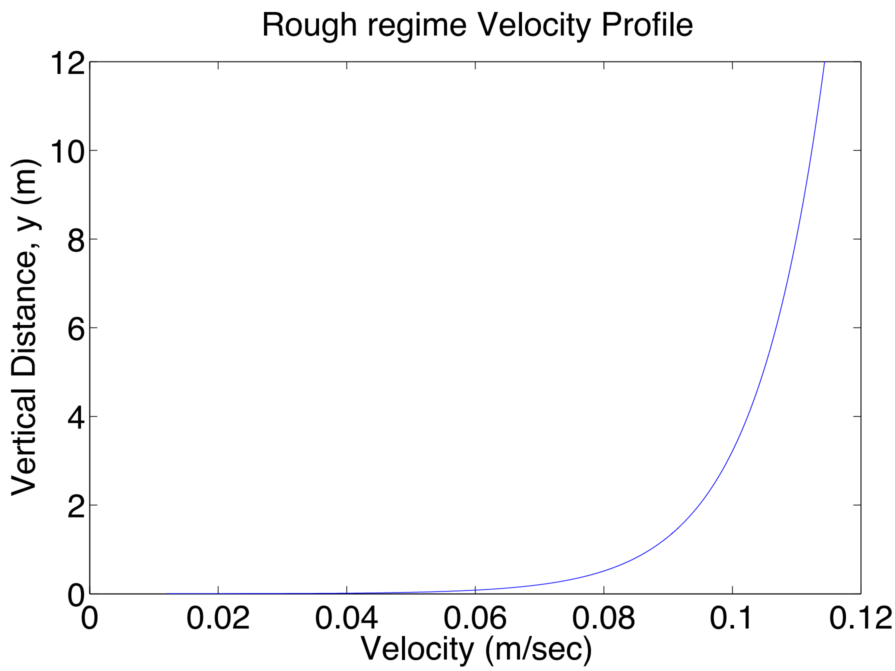

Figure 2.3: Rough Regime Velocity Profile.

2.2.3 Numerical equations

Once the velocity profiles are calculated they can be implanted in the transport model. A **2D Lagrangian Particle Tracking Method (LPTM)** has been developed which represents a **random walk problem**.

For the tracking of the algae plants in the intake filtering channel the equations introduced in section 2.1.2 are used accordingly. Thus in the case of a constant diffusivity, D, along the vertical direction, the equations for the case of an open channel may be written as:

$$x_{t+\Delta t} = x_t + u(y)\Delta t \tag{2.2.3}$$

$$y_{t+\Delta t} = y_t + \xi\sqrt{2D\Delta t} \tag{2.2.4}$$

where x is the streamwise direction, y the vertical distance from the bed of the channel, $u(y)$ the calculated velocity profile imposed in the transport model and Δt the timestep. The above equations describe the behaviour of the algae plants (or particles) under the influence of advection in the streamwise direction and diffusion in the vertical direction. So the advective movement of the particle is superimposed by a random movement in the vertical direction that represents turbulent diffusion [6]. This random movement lies in the properties of ξ, which is a normal distributed number with a mean quantity of zero and a variance equal to one. The diffusive term describes the spreading of the particles in the vertical direction relative to the release point as the particles progress in the streamwise direction. Figure 2.4 shows the random vertical displacements followed by a particle released at the origin (0,0) between successive timesteps.

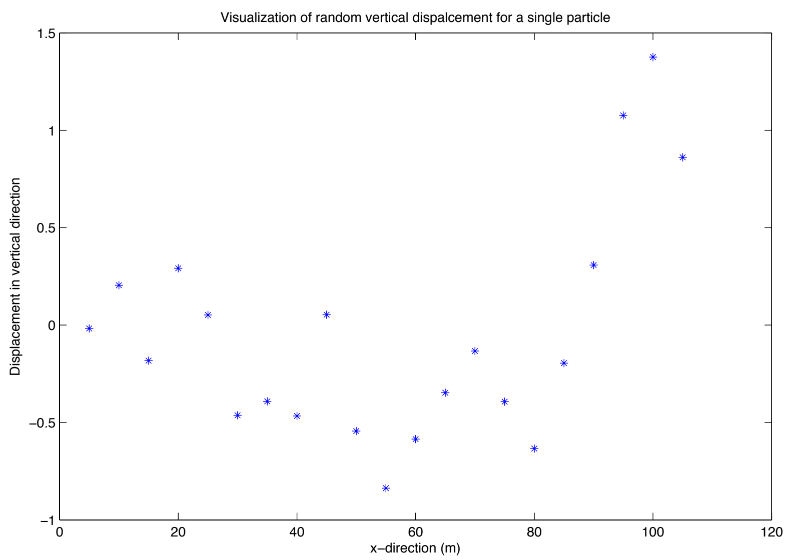

Figure 2.4: Visualization of random displacement in vertical direction between time steps.

The individual algae plants are modelled as small spheres. The important feature of the simulation is the tracking of a sufficient large number of discrete particles (i.e of the individual algae plants). As the number of particles increases the accuracy of the Lagrangian approach also increases which makes this approach suitable for the demands of the project.

Considering now the case of a variable diffusivity, $D(y)$ in the vertical direction, the equations become:

$$x_{t+\Delta t} = x_t + u(y)\Delta t \tag{2.2.5}$$

$$y_{t+\Delta t} = y_t + \left[\frac{dD(y)}{dy}\right]_{y=y_t} \Delta t + \xi\sqrt{2D(y(t))\Delta t} \tag{2.2.6}$$

Note that in this case the correction proposed by I$\hat{t}$o was included. This term as mentioned before is called the *noise induced drift component* and suitable simulations were performed in order to assess its effect on the model developed. The effect of the random step in the streamwise direction representing turbulent diffusion was not included here; its effect on the developed model is further investigated in chapter 4.

2.2.4 Boundary conditions

In the model developed the necessary boundary conditions are determined by the bed and the free surface of the channel. The surface of the channel is an impermeable boundary and no flux condition is imposed. But this condition can be violated by the overshooting of the trajectories of the simulated algae plants, when the stochastic displacement in the vertical direction is too large. To overcome this problem, apart from making the timestep small, a simple approach is used which considers the boundary as a reflective one. Doing so the particle will be reflected back into the domain of the simulation by the the amount it penetrates into the boundary domain, as shown by figure 2.5. The same treatment is applied for the bed of the channel [7].

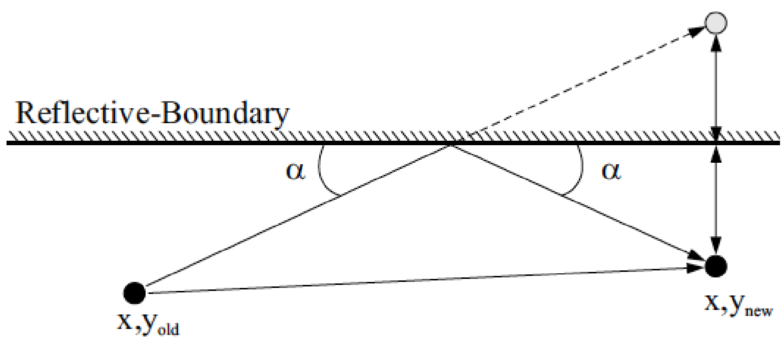

Figure 2.5: Reflecting boundary.

2.2.5 Forces on algae plants

The code was extended to account for buoyant forces acting on the algae plants due to density differences. The method used as well as the results obtained from the simulations are presented and discussed further in section 3.1.4.
The algae plants are modelled as spherical particles, as their actual shape is very complex to model. An assumption of the effective diameter of the modelled spherical algae plant is made and this is $d_{plant} = 2\ mm$. All of the mass of the actual algae plant is assumed to be uniformly distributed over a sphere with the effective diameter just mentioned.

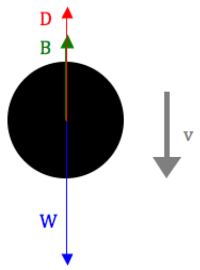

Figure 2.6: Forces on a spherically modelled algae plant.

Considering the forces acting on a spherically modelled algae plant and applying a force balance:

$$\Sigma f = ma$$
$$B - W + D = ma$$
$$\frac{\rho_f g \pi d^3}{6} - \frac{\rho_a g \pi d^3}{6} + \frac{\rho_f C_d \pi d^2 v^2}{8} = m\frac{dv}{dt}$$

Assuming the algae plant has reached its terminal speed,

$$\frac{dv}{dt} = 0$$

Solving for v will give the terminal velocity v_{term} to be:

$$v_{term} = \sqrt{\frac{4gd(\rho_a - \rho_f)}{3\rho_f C_d}} \tag{2.2.7}$$

At this point an assumption is made of creeping flow ($Re < 1$) and for this case the drag coefficient is $C_d = 24/Re$ [8].
In order to verify the assumption of creeping flow the drag coefficient, C_d, is substituted in equation 2.2.7 which yields the so called *Stokes velocity* which is equal to :

$$v_{stokes} = \frac{gd^2(\rho_a - \rho_f)}{18\mu_f} \tag{2.2.8}$$

The density of the algae plants is very close and in particular slightly higher to the density of the water [9]. An assumption is made for this density so that $\rho_a = 1010\ kg/m^3$.
In estimating the fall velocity a need arises to verify the previous assumption made of creeping flow. Therefore the Reynolds number is calculated. The Reynolds number calculated does not confirm a creeping flow. The Reynolds number found is $Re = 122.7$ and the condition for creeping flow is that $Re < 1$. The following iterative solution is considered in order to derive the fall velocity.
Using the Reynolds number calculated the drag coefficient is calculated based on the empirical approximation : $C_d = 24/Re + 3/\sqrt{Re} + 0.34$.
This gives $C_d = 0.806$ which is used in 2.2.7 an so a new estimation of the fall velocity is made, this is $v_{term} = 4.86 \times 10^{-4}\ m/sec$. A new Reynolds number is calculated from this giving $Re_{new} = 1.326$. The new value obtained for the Reynolds number is far off the previous value and so the iteration must continue in a similar manner until the old and the new Reynold numbers are within 10 percent of eachother.

The iteration results are shown on table 2.1 below. From the iteration the terminal velocity is estimated to be equal to **0.0173** m/sec.

Table 2.1: Iteration for terminal velocity

Re_{old}	C_d	v_{term}	Re_{new}
1.33	21.04	0.0043	11.78
11.78	3.25	0.0110	29.96
29.96	1.69	0.0152	41.57
41.57	1.38	0.0168	45.94
45.94	1.31	0.0173	47.29

2.2.6 Band screen and Wash-water system

The band screen is an endless 'belt' of mesh panels contained within a vertical self-supporting steel frame. The mesh panels are of woven wire (of 1 mm thickness) and each is supported on a steel frame. The debris is collected on the outside of the mesh and is lifted above deck level, as the band screen rotates, and is washed off into a debris gully by the wash-water system.
The wash-water system consists of an independent wash-water supply provided to each band screen by a submerged pump situated on the discharge side of the band screen. The pump is connected to a strainer and then this to the jetpipes which clean the mesh panels of the band screen. The operating pressure is 1.7 bar.

2.2.7 Band screen control and Differential levels

A differential level equipment installed measures the differential level across the band screen. If this differential rises to 300 mm, the screen will start on low speed and when the differential falls to 200 mm the screen will stop. When the differential across the screen rises to 400 mm, instead of dropping, then the screen will change to high speed and will return back to low speed when the differential drops to 300 mm. A high differential alarm is initiated if the differential rises to 500 mm and should the differential continuous to rise a shut down is initiated at 575 mm differential. The maximum screen design differential is 600 mm.

2.2.8 Model for interaction of algae plants with the band screen

The 2-D model developed is further extended in order to account for the interaction of the algae plants with the grid of the mesh panels of the band screen.
The effective opening (i.e the opening through which water can pass) between the wires of the mesh when the screen is clean is s=5 mm and the wires are d=1 mm thick. The model considered is shown by figure 2.7. The algae plants can bend due to their flexibility and so it is assumed that a fraction of them will be able to pass through the filter even though they are larger in reality than the spacing between the wires of the mesh. To model this effect two lengths are defined, l_p and l_b, the opening and blockage length respectively. An algae plant with its centre positioned within the opening length will pass through the mesh grid of the screen whereas an algae plant positioned within the blockage length will be blocked and attach to the screen. The model assumes that only these defined parameters determine if an algae plant will pass through the screen or attach to it, and no interaction between the individual algae plants is considered. This method was adopted in the code

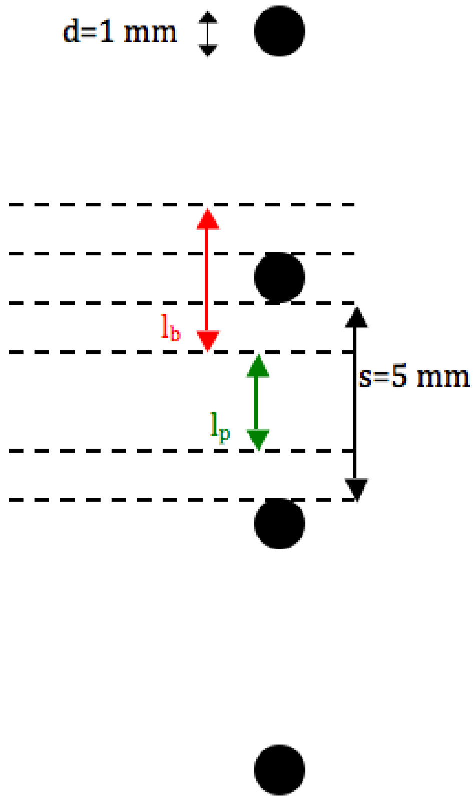

Figure 2.7: Model used for the interaction of the algae plants with the mesh panels of the band screen.

for modelling the effect of the algae plants flexibility. Simulations were made in order to assess the impact of this effect on the screening. The model calculates the vertical positions of the algae plants at the point in the streamwise direction where the band screen is located (at x=15 m from the start of the channel where the plants are released), and the number of the algae plants blocked and passing though the screen are calculated based on the values of l_p and l_b chosen.

Chapter 3

Algae plants trajectories in the intake channel

3.1 Simulations: Results and Discussion

In the simulations that follow the algae plants are released at the start of the channel, $x = 0\ m$, and are uniformly distributed over the depth of the channel h.

3.1.1 Linear velocity profile

Initially a simulation using the developed model is made for the case of a linear velocity profile. The parameters used in the simulation are shown on table 3.1.

Table 3.1: Simulation Parameters

Parameter	Value
Number of algae plants	5000
Depth of channel, h (m)	1
Diffusion coefficient, D (m^2/sec)	0.01
Timestep, Δt (sec)	0.01
Velocity profile, u (m/sec)	$U\frac{y}{h}$

On the left column of figure 3.1 the calculated positions of the algae plants at different time steps are shown. The plants follow the linear velocity profile imposed in the transport model and are advected in the streamwise direction and also diffuse in the vertical direction. Figures 3.1(g) and 3.2 show that the plants are well mixed after travelling a large distance in the streamwise direction and the linear velocity profile is smeared out. The concentration of the plants reaches a Gaussian distribution after 100000 time steps as shown by figure 3.3. The results obtained are consistent with similar LPTM simulations by Weitbrecht (2003) shown on the right column of figure 3.1.

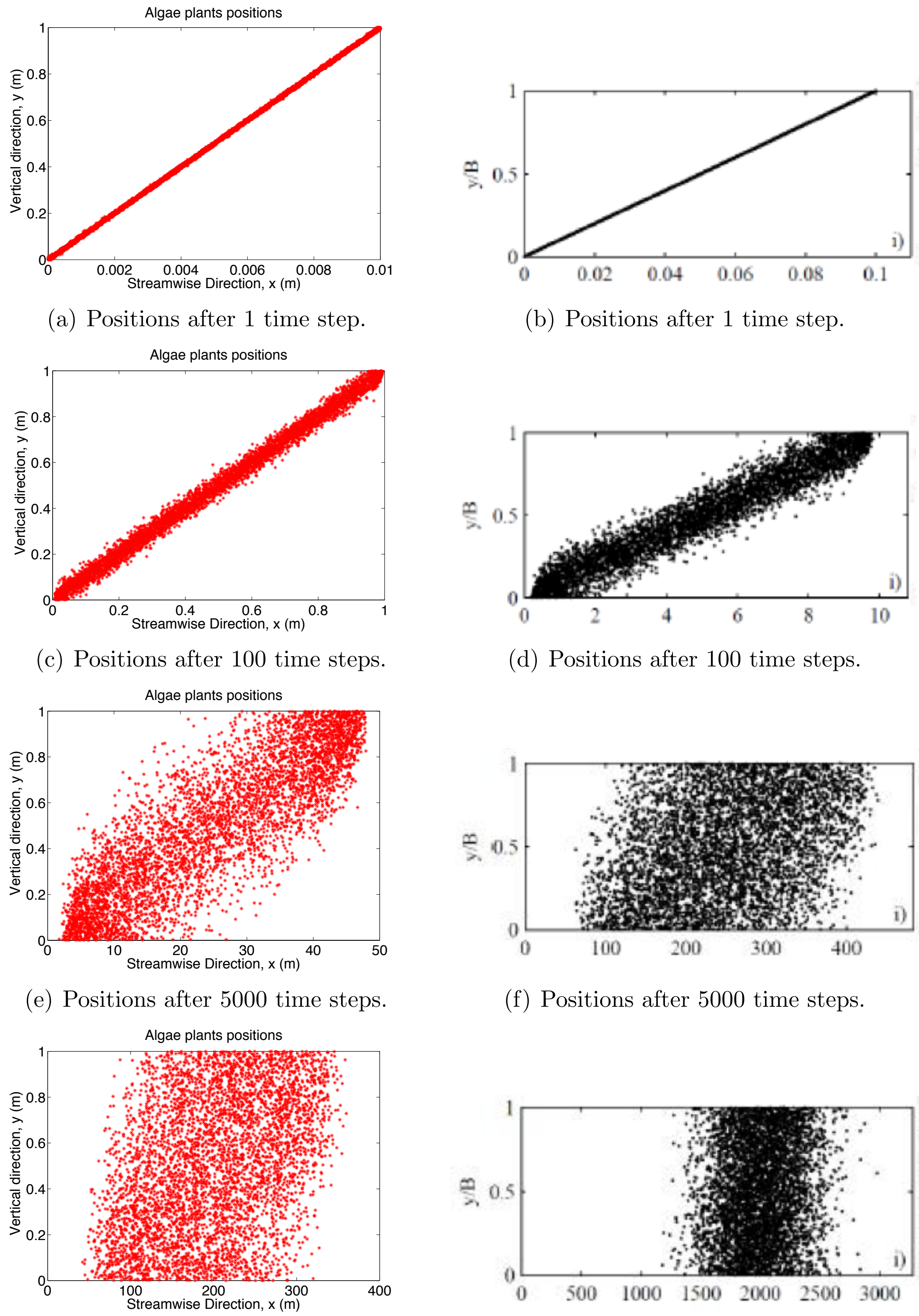

(a) Positions after 1 time step.
(b) Positions after 1 time step.
(c) Positions after 100 time steps.
(d) Positions after 100 time steps.
(e) Positions after 5000 time steps.
(f) Positions after 5000 time steps.
(g) Positions after 40000 time steps.
(h) Positions after 40000 time steps.

Figure 3.1: Linear velocity profile simulation at different time steps showing the positions of the algae plants. Right column shows LPTM simulations by Weitbrecht (2003) for also a linear velocity profile.

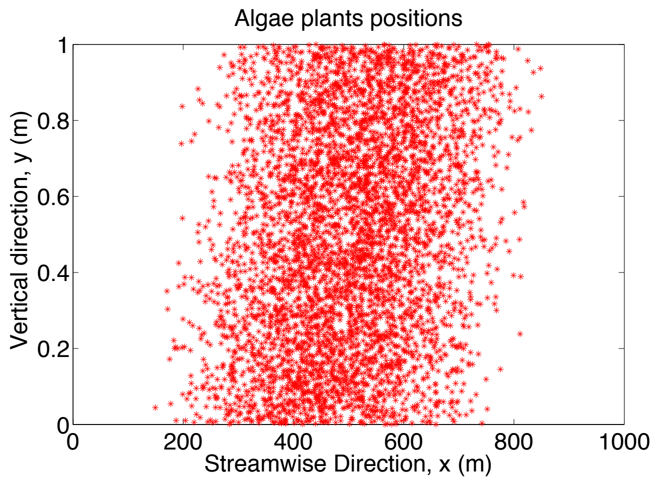

Figure 3.2: Positions of algae plants after 100000 time steps.

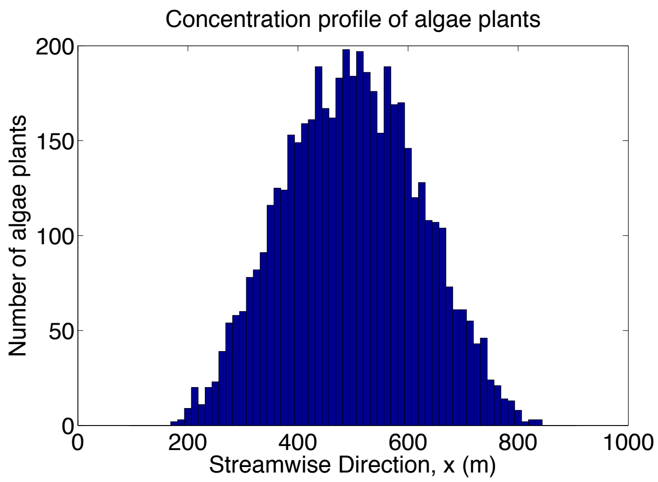

Figure 3.3: Concentration profile of algae plants after 100000 time steps.

3.1.2 Logarithmic velocity profile with constant diffusivity

The bed of the channel is smooth so the logarithmic velocity profile for a smooth regime is used. The diffusion coefficient in this case has been chosen to be constant with a value according to Fischer et al. (1979) for regular channels. The parameters of the simulation are shown on table 3.2. Figure 3.4 shows the positions of the algae plants at different time steps. From figures 3.4(b), 3.4(c) and 3.4(d) a front of higher concentration near the surface is observed. This is because the velocity profile gradient close to surface is less steep compared to when close to the bed of the channel and so this leads to a slower mixing of the plants. After 100000 time steps though the logarithmic velocity profile is smeared out and also the higher concentration front is smoothed out resulting in an almost Gaussian distribution of the plants around a mean, as in the case observed for a linear velocity profile.

Table 3.2: Simulation Parameters

Parameter	Value
Number of algae plants	5000
Depth of channel, h (m)	1
Diffusion coefficient, D (m^2/sec)	$0.15u_*h$
Timestep, Δt (sec)	0.01
Velocity profile, $\bar{u}(y)$ (m/sec)	Eq. 2.2.1

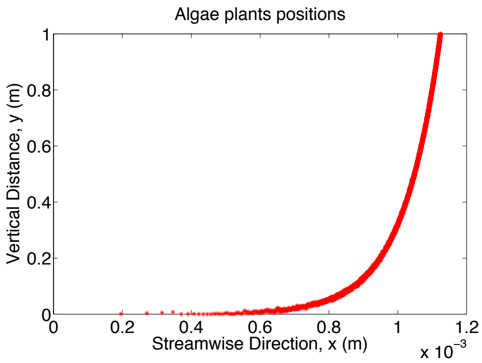

(a) Positions after 1 time step.

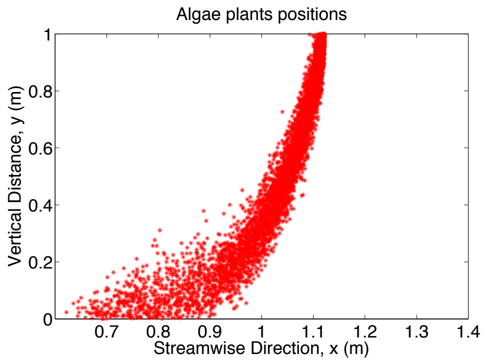

(b) Positions after 1000 time steps.

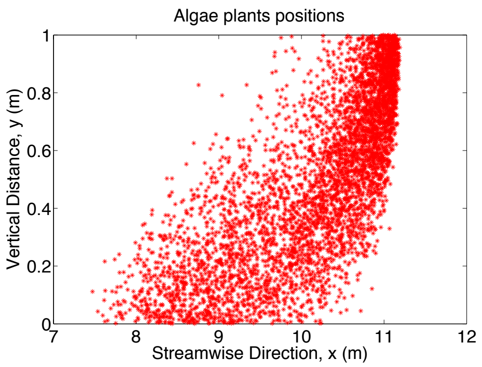

(c) Positions after 10000 time steps.

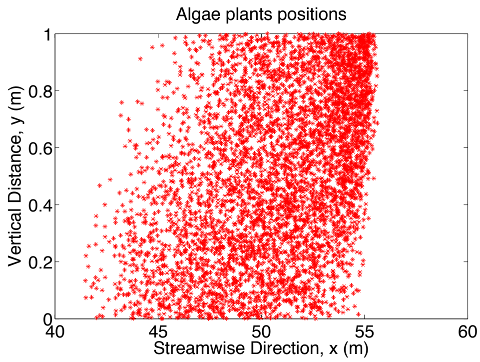

(d) Positions after 50000 time steps.

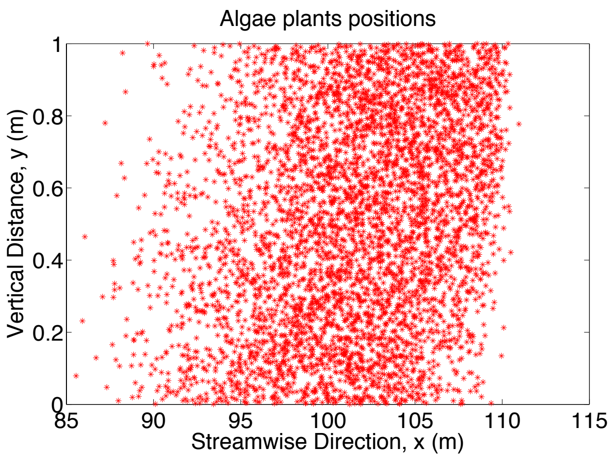

(e) Positions after 100000 time steps.

Figure 3.4: Logarithmic velocity profile simulation for smooth regime with constant diffusivity showing the positions of the algae plants for different time steps.

3.1.3 Logarithmic velocity profile with varying diffusivity

The model is now used to simulate the case when the diffusivity is varying. Again a logarithmic velocity profile in the smooth regime is used. The parameters of the simulation are given on table 3.3. The diffusivity varies in the vertical direction and is set to be equal to the analytical result of Elder (1959)[6].

Table 3.3: Simulation Parameters

Parameter	Value
Number of algae plants	5000
Diffusion coefficient, $D(y)$ (m^2/sec)	$\kappa u_* y(1 - y/h)$
Timestep, Δt (sec)	0.01
Drift component, $dD(y)/dy$	$\kappa u_*(1 - 2y/h)$
Velocity profile, $\bar{u}(y)$ (m/sec)	Eq. 2.2.1

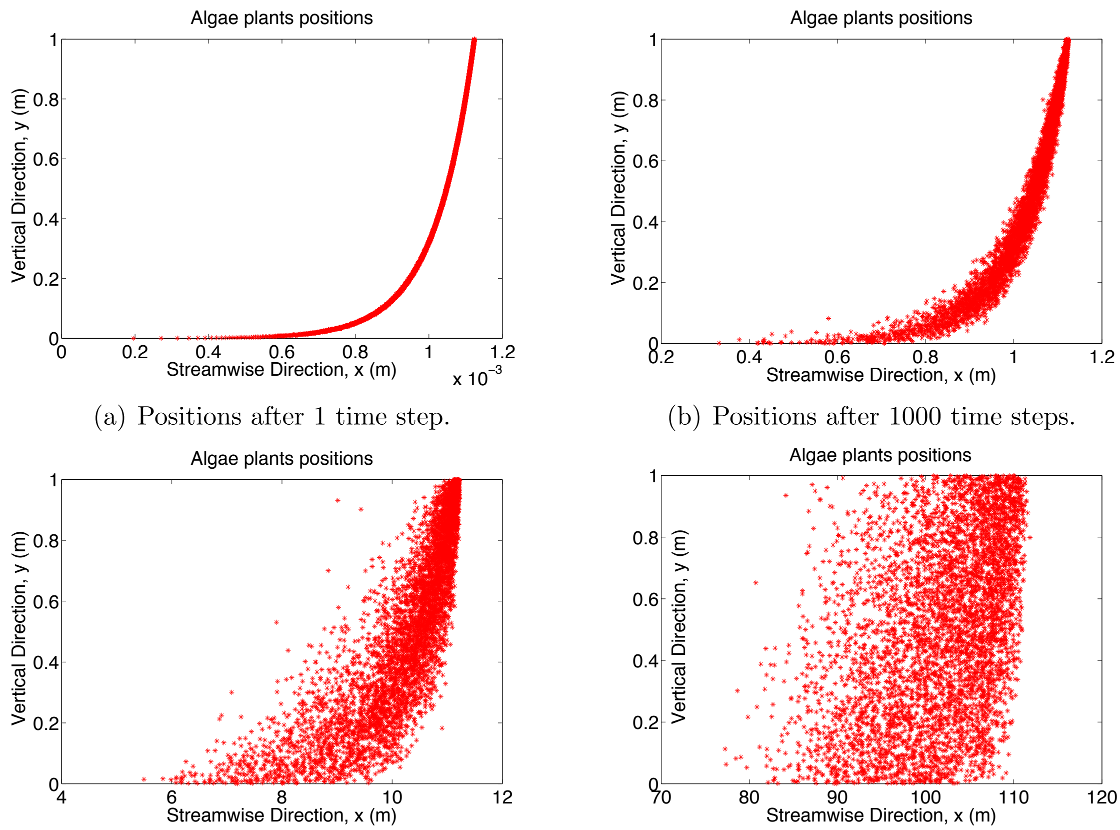

(a) Positions after 1 time step.

(b) Positions after 1000 time steps.

(c) Positions after 10000 time steps.

(d) Positions after 100000 time steps.

Figure 3.5: Logarithmic velocity profile simulation for smooth regime with varying diffusivity and including the noise induced drift component.

The above simulation was made under the parameters of Elder's analytical solution. The logarithmic velocity profile is visible in figures 3.5(a), 3.5(b) and 3.5(c). The results of figure 3.5(d) show a good mixing of the algae plants and the logarithmic velocity profile has almost smeared out.

Comparing this simulation with the the simulation is section 3.1.2 we observe that mixing in this case in not as strong, suggesting that the local diffusivity values in this case are lower than the constant diffusivity used earlier.

A further simulation is made under the same parameters for the case when increasing the time steps enough so that the velocity profile is completely smoothed out. Also the concentration profile was calculated and is shown by figure 3.7(b), from the results we see that the concentration of the plants is almost Gaussian suggesting an even mixing of the algae plants around a mean. The results obtained are compared to a similar LPTM model which also uses Elders analytical solution. The results are similar and consistent with eachother, in both calculating the positions of the particles as well as the concentration profiles. This comparison validates and verifies the model developed for the purposes of this project.

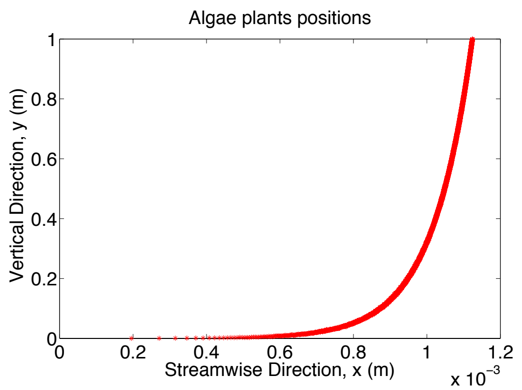

(a) Positions of algae plants after 1 time step.

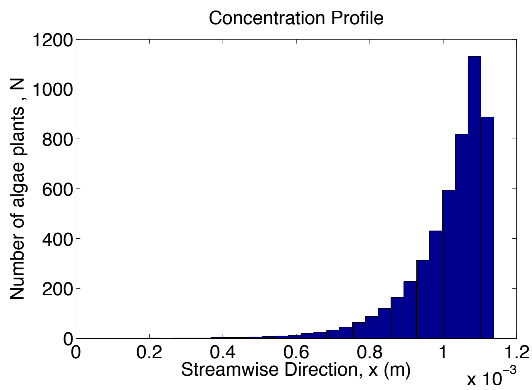

(b) Concentration profile of algae plants after 1 time step.

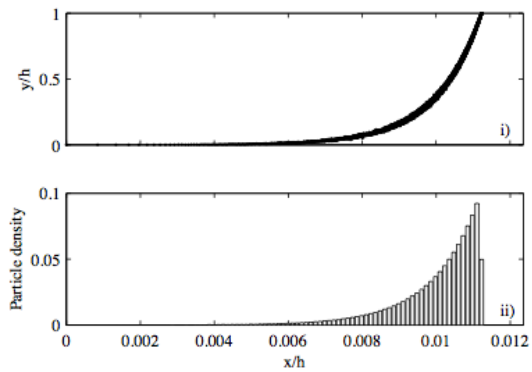

(c) Adopted from [6] showing an LPTM simulation based on Elder's analytical solution. Particles positions after 1 time step and concentration profile.

Figure 3.6: Comparison of LPTM simulations based on parameters of Elder's analytical solution.

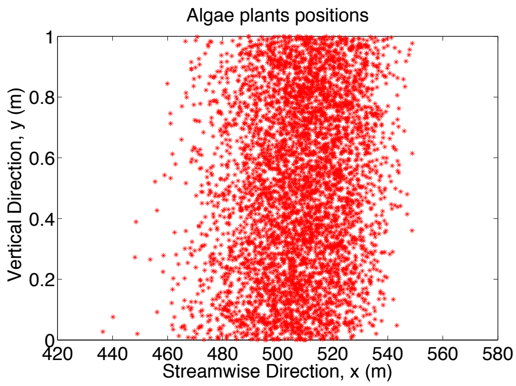

(a) Positions of algae plants after 5×10^5 time steps.

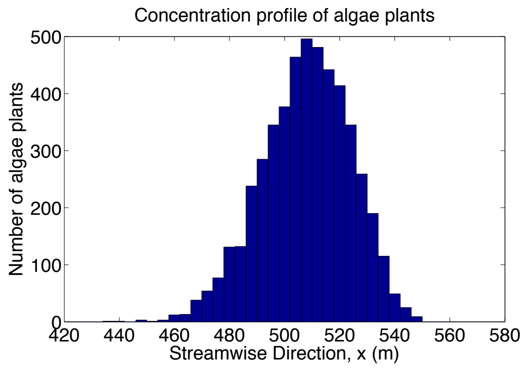

(b) Concentration profile of algae plants after 5×10^5 time steps.

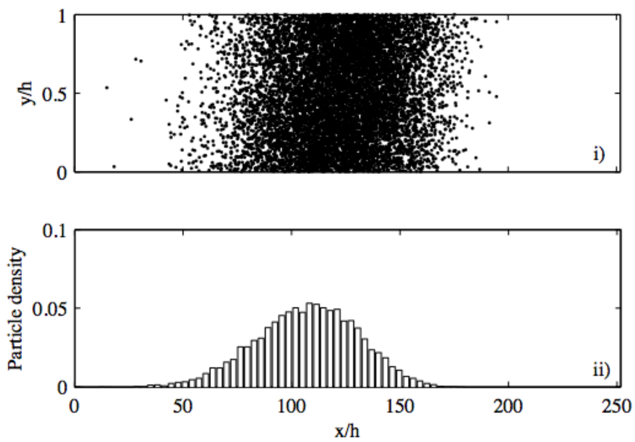

(c) Adopted from [6] showing an LPTM simulation based on Elder's analytical solution. Particles positions after 1×10^5 time steps and concentration profile.

Figure 3.7: Comparison of LPTM simulations based on parameters of Elder's analytical solution.

Effect of noise induced drift component

In order to verify the effect of the noise induced drift component, as discussed in 2.1.2, the same simulation was made under the same parameters but the drift component was not included.

The results of this simulation are shown by figure 3.8. From the results obtained its shown that the particles tend to move in regions of low diffusivity and thus accumulate near the bed of the channel (figures 3.8(c) and 3.8(d)). The effect of the noise induced drift component is obvious when comparing figures 3.9 to 3.10 and 3.11 to 3.12. These show the concentration profiles for the two different cases discussed above. Note how the algae plants accumulate near the bed at high concentrations, where the local values of the diffusivity are low, when the drift component is omitted. The correction term by I$\hat{t}$o has the effect of redistributing these plants along the whole depth of the channel. The concentration profiles when including the noise induced drift component have approximately the same number of algae plants at each position along the depth of the channel. Some discrepancies do exist but the overall result is more reasonable than the case when the drift component was not included.

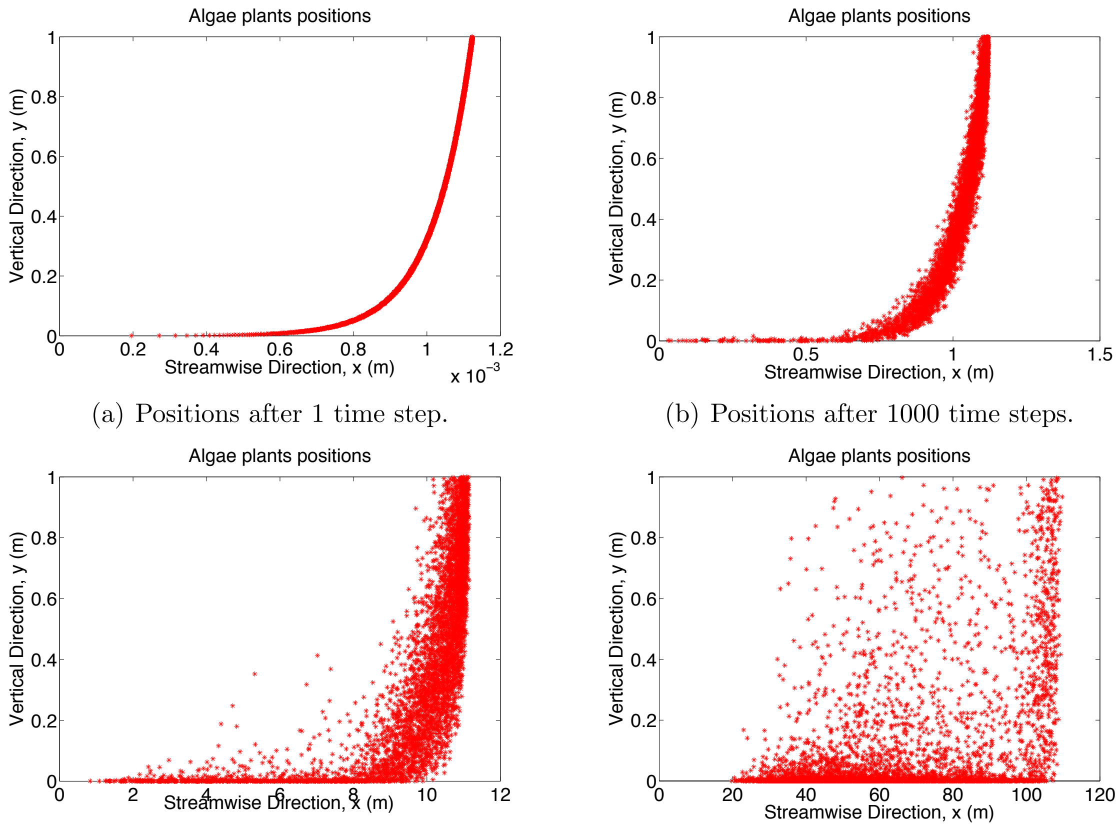

(a) Positions after 1 time step.

(b) Positions after 1000 time steps.

(c) Positions after 10000 time steps.

(d) Positions after 100000 time steps.

Figure 3.8: Logarithmic velocity profile with varying diffusivity not including the noise induced drift component.

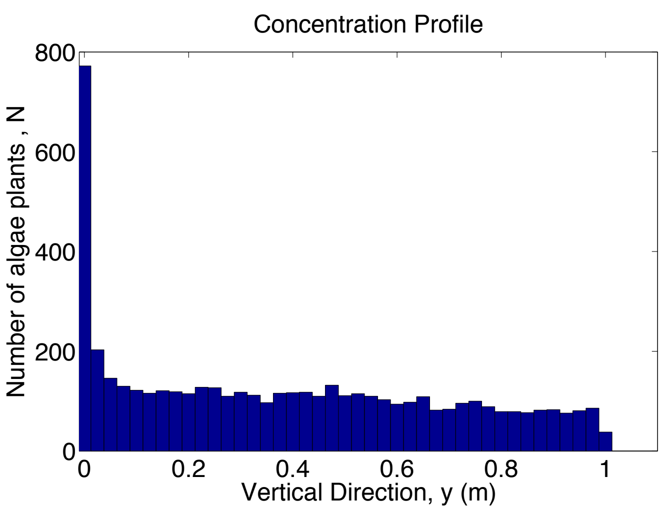

Figure 3.9: Concentration profile of algae plants after 10000 time steps not including the noise induced drift component.

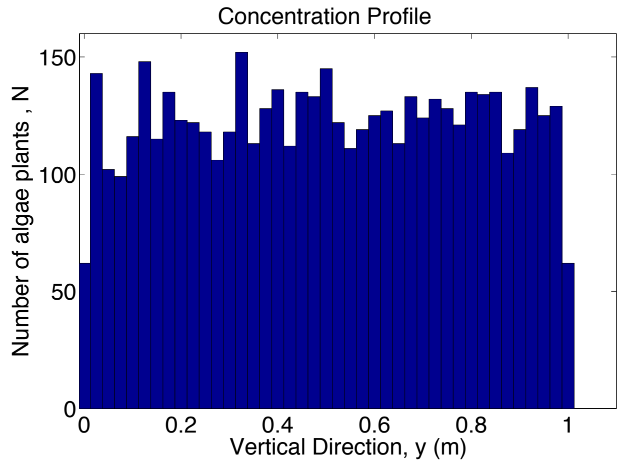

Figure 3.10: Concentration profile of algae plants after 10000 time steps including the noise induced drift component.

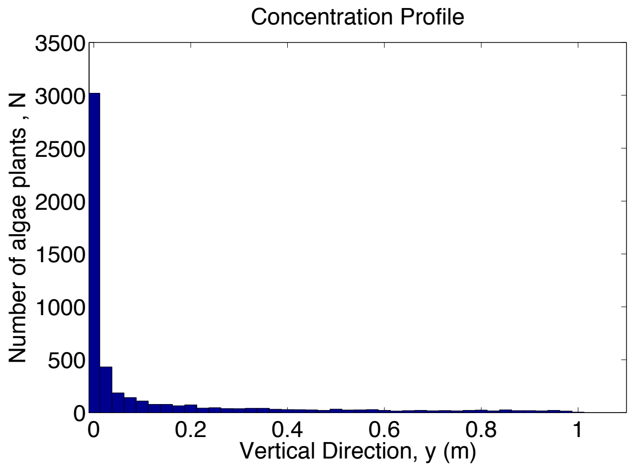

Figure 3.11: Concentration profile of algae plants after 100000 time steps not including the noise induced drift component.

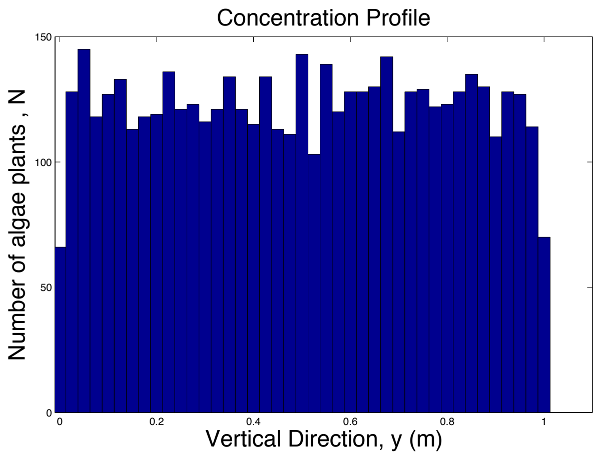

Figure 3.12: Concentration profile of algae plants after 100000 time steps including the noise induced drift component.

3.1.4 Logarithmic velocity profile with varying diffusivity and including the fall velocity

The simulation shown by figure 3.13 was made so that the effect of the fall velocity on the algae plants could be investigated. The parameters of this simulation are shown on table 3.4.

The slightly higher density of the algae plants will cause them to sink as discussed in 2.2.5 and so the fall velocity causes a downward displacement on the algae plants forcing them to move towards the bed of the channel .

After one time step this effect is not visible and the algae plants follow as usual the logarithmic velocity profile as usual (figure 3.13(a)).

For 1000 time steps, figure 3.13(b), we still cannot see any effect on the trajectories of the algae plants. The effect of the fall velocity is starting to appear after 10000 time steps have passed as shown by figure 3.13(c). The algae plants have started accumulating on the bed of the channel and finally after 50000 time steps we can see from figure 3.13(d) that the algae plants clearly follow a sinking trajectory and many have accumulated on the bed.

The algae plants that were initially uniformly distributed across the whole depth of the channel cover now only three quarters of the same depth with a few algae plants being within a distance of 3 m below the surface of the water. The concentration of the algae plants increases with distance from the surface and reaches a maximum at the bed of the channel.

Table 3.4: Simulation Parameters

Parameter	Value
Number of algae plants	5000
Diffusion coefficient, $D(y)$ (m^2/sec)	$\kappa u_* y(1 - y/h)$
Depth of channel, (m)	12
Timestep, Δt (sec)	0.01
Drift component, $dD(y)/dy$	$\kappa u_*(1 - 2y/h)$
Fall velocity, w (m/sec)	0.0173
Velocity profile, $\bar{u}(y)$ (m/sec)	Eq. 2.2.1

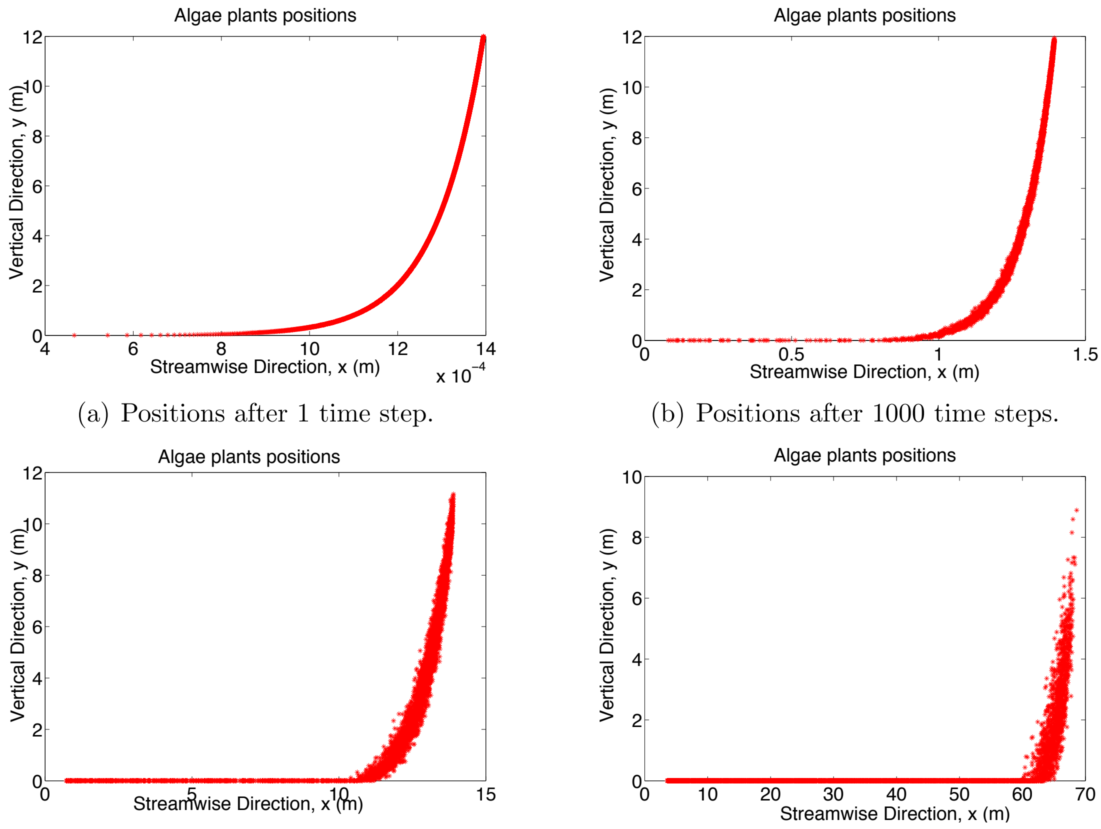

(a) Positions after 1 time step.

(b) Positions after 1000 time steps.

(c) Positions after 10000 time steps.

(d) Positions after 50000 time steps.

Figure 3.13: Positions of algae plants for a logarithmic velocity profile in the smooth regime with varying diffusivity, including the noise induced drift component and the fall velocity.

3.2 Continuous release from bed of channel

Previously it was shown that the fall velocity caused the algae plants to concentrate at the bed of the channel after travelling a long distance in the streamwise direction. An investigation is now made for the case of the entrainment of the algae plants from a loose channel bed.

The difference of this simulation to the previous simulations is that the release is now continuous and the algae plants are uniformly distributed and released along the bed of the channel rather than along the depth of the channel. Similar simulations concerning the entrainment of sediment transport from the bed of a channel show that the concentration profiles of suspended sediment follow the trend shown by figure 3.18 [10]. It is expected that a similar trend should occur for the case of the concentration of the entrained algae plants.

The parameters used for this simulation are summarised on table 3.5.

These parameters used are the same as the conditions of the original entrainment experiment by Van Rijn (1986). Figures 3.14, 3.15, 3.16 and 3.17 show the implementation

Table 3.5: Simulation Parameters for continuous release from bed of channel

Parameter	Value
Number of algae Plants (per release)	1000
Depth of channel, $h(m)$	0.25
Length of release, (m)	10 $(40h)$
Number of releases, N	20
Timestep, Δt (sec)	0.01
Drift component, $dD(y)/dy$	$\kappa u_*(1-2y/h)$
Diffusion coefficient, $D(y)$ (m^2/sec)	$\kappa u_* y(1-y/h)$
Fall velocity, w (m/sec)	0.022
Mean velocity, $\bar{U}(m/sec)$	0.67
Nikuradse roughness, $k_s(m)$	0.01
Friction velocity, u_* (m/sec)	0.047
Velocity profile, $\bar{u}(y)$ (m/sec)	Eq. 2.2.2

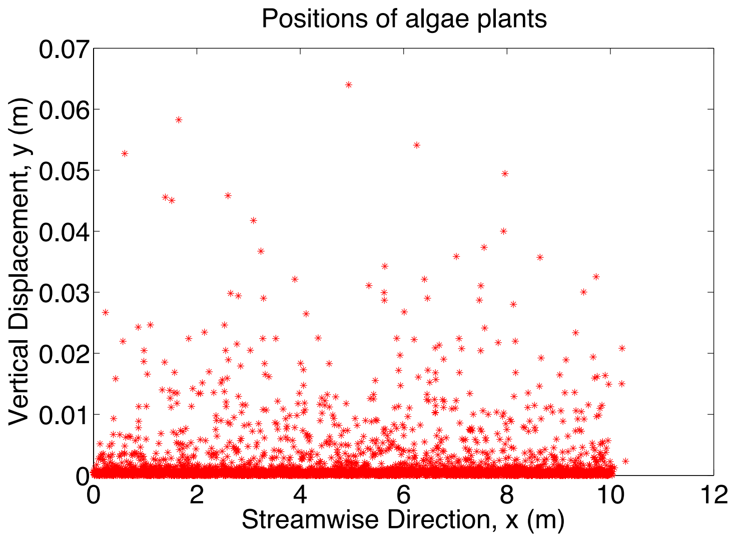

Figure 3.14: Positions after 100 time steps.

of the continuous release and its evolution at different time steps. In this simulation 1000 plants uniformly distributed along the bed between $0\ m < x < 10\ m$ are released every 50 time steps. At the end of the simulation a total of 20000 alga plants are released in the channel. The concentration profiles of unit length water columns were computed and are shown by figure 3.19 . From the results we see that the entrained algae plants concentration profiles follow a similar trend to suspended sediment concentration profiles; this demonstrates that the model represents well the physical processes involved. Also all of the computed concentration profiles are similar even though they correspond to different water columns along the streamwise direction, this indicates that the concentration profiles are fully developed and independent of the streamwise direction.

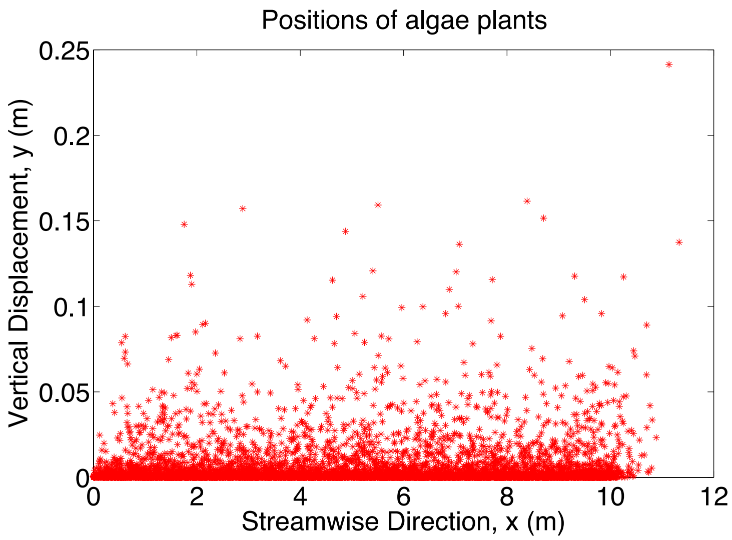

Figure 3.15: Positions after 300 time steps.

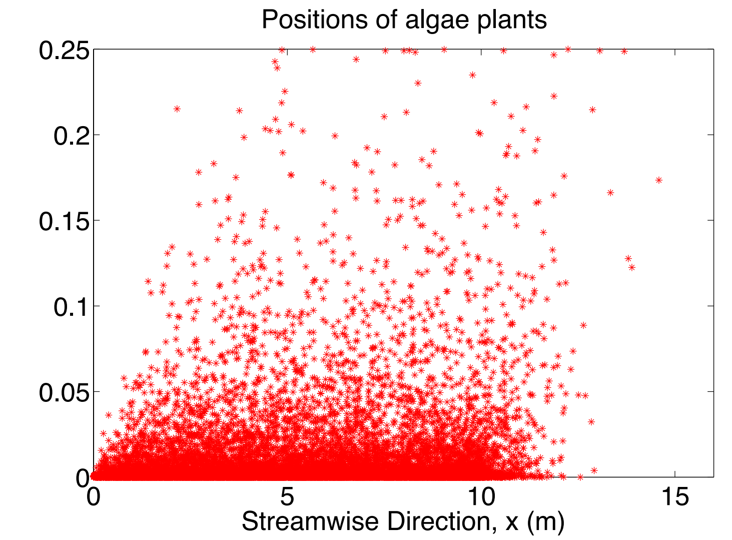

Figure 3.16: Positions after 700 time steps.

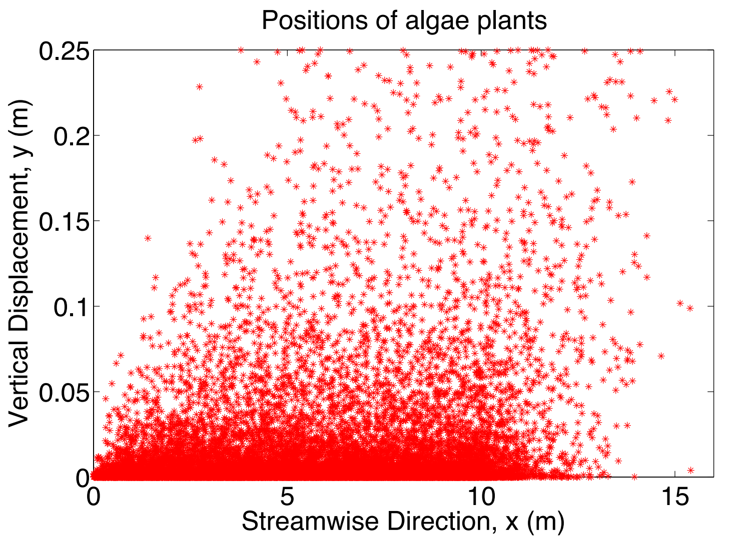

Figure 3.17: Positions after 1000 time steps.

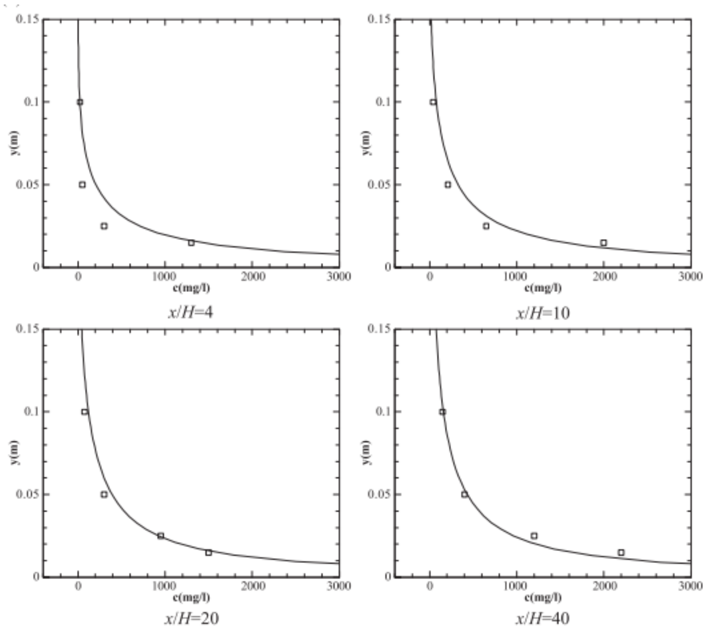

Figure 3.18: Adopted from [10].Comparison of the predicted (solid lines) and measured (squares) suspended sediment concentrations.

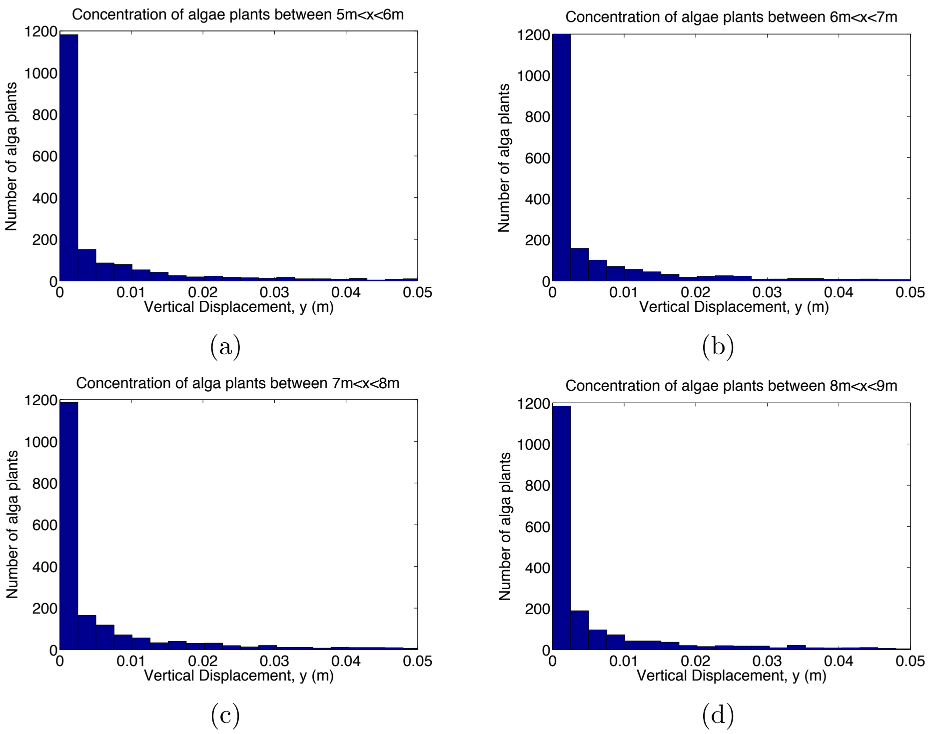

Figure 3.19: Concentration of algae plants of different unit length water columns for a continuous release from the bed of the channel.

Chapter 4

Impact of diffusion in the streamwise direction

The numerical equations used so far have considered only advection in the streamwise direction and a random step was used to represent turbulent diffusion in the vertical direction. Now the effect of a similar random step to represent turbulent diffusion in the streamwise direction is investigated. Therefore the numerical equations considered in this case are:

$$x_{t+\Delta t} = x_t + u(y)\Delta t + \xi\sqrt{2D_x\Delta t} \tag{4.0.1}$$

$$y_{t+\Delta t} = y_t + \left[\frac{dD(y)}{dy}\right]_{y=y_t} \Delta t + \xi\sqrt{2D(y(t))\Delta t} \tag{4.0.2}$$

where all symbols are the same as discussed section 2.2.3 and D_x is the diffusion coefficient in the streamwise direction. The diffusion coefficient in the streamwise direction is constant and it is assumed to be equal to its transverse counterpart, hence it is equal to $D_x = 0.15hu_*$.

The simulations of sections 3.1.3 and 3.1.4 are reproduced here but the new numerical equations are used. The parameters of the simulations are the same as before and can be found on the corresponding tables in each of the above mentioned sections.

4.1 Logarithmic velocity profile with varying diffusivity

Comparing the new simulation results of figure 4.1 to figure 3.5 the differences are obvious. After one time step the diffusive random step in the streamwise direction is larger than the advective component and thus the logarithmic velocity profile is not visible. For 1000 time steps the velocity profile can now be seen and comparing figures 4.1(b) and 3.5(b) the mixing of the algae plants in the streamwise direction is significantly stronger even though the distances travelled are similar. The effect of the streamwise diffusion starts to diminish after 10000 time steps, the mixing of the plants in figures 4.1(c) and 3.5(c) is approximately the same with the difference that the higher concentration front near the surface observed in figure 3.5(c) is in this case less obvious. Also now the plants have travelled slightly further in the channel. Finally after 100000 time steps the effect of the random step in the streamwise direction is not visible as in both cases, shown by figures 4.1(d) and 3.5(d), the range of mixing of the plants along the streamwise direction is the same which implies advection is the dominant process.

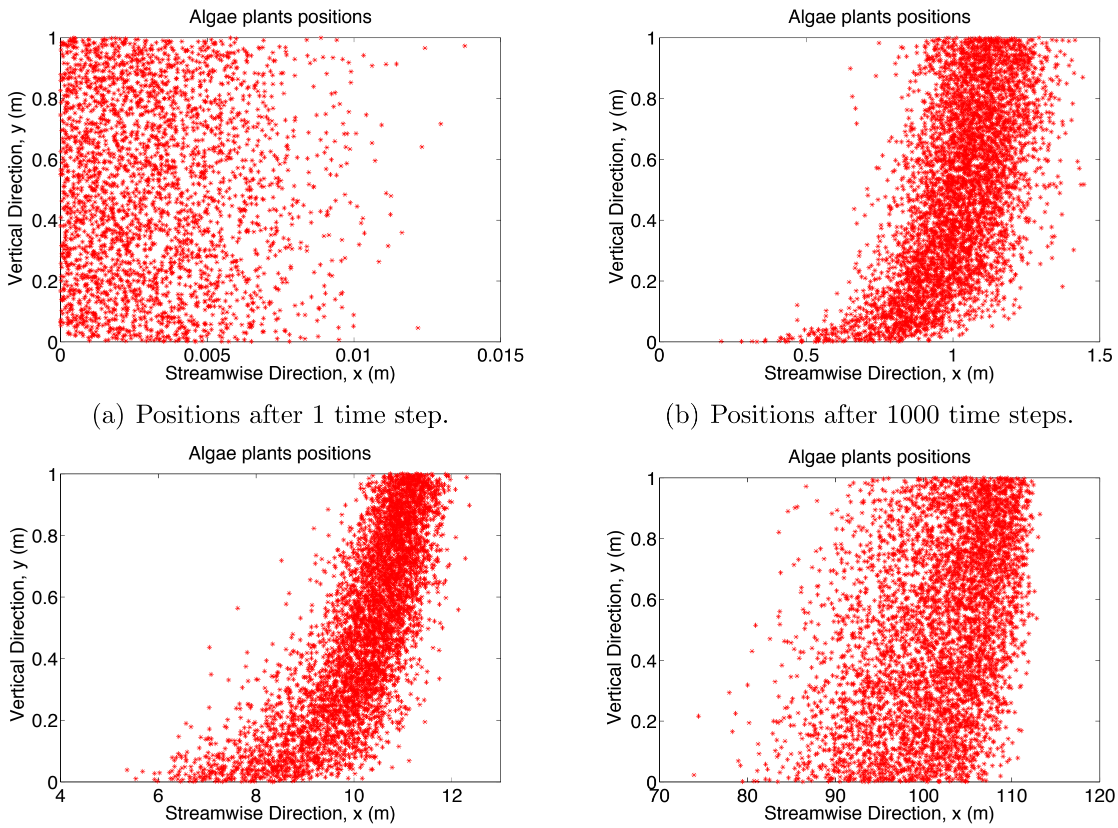

(a) Positions after 1 time step.

(b) Positions after 1000 time steps.

(c) Positions after 10000 time steps.

(d) Positions after 10000 time steps.

Figure 4.1: Positions of the algae plants for a logarithmic velocity profile in the smooth regime with varying diffusivity, including the noise induced drift component and diffusion in the x-direction.

4.2 Logarithmic velocity profile with varying diffusivity and including the fall velocity

In this simulation the full depth of the intake channel is considered as well as the fall velocity on the algae plants. The results are shown by figure 4.2. Comparing with the results shown by figure 3.13 a much stronger mixing in the streamwise direction is now observed. The effect of the diffusive step is strong and visible in all of the timesteps shown. The same observations apply as discussed previously but now the diffusion coefficient is greater as the depth of the channel has increased. After a sufficient large number of time steps has passed advection is expected to dominate, of course in this case the algae plants will accumulate on the bed by then.

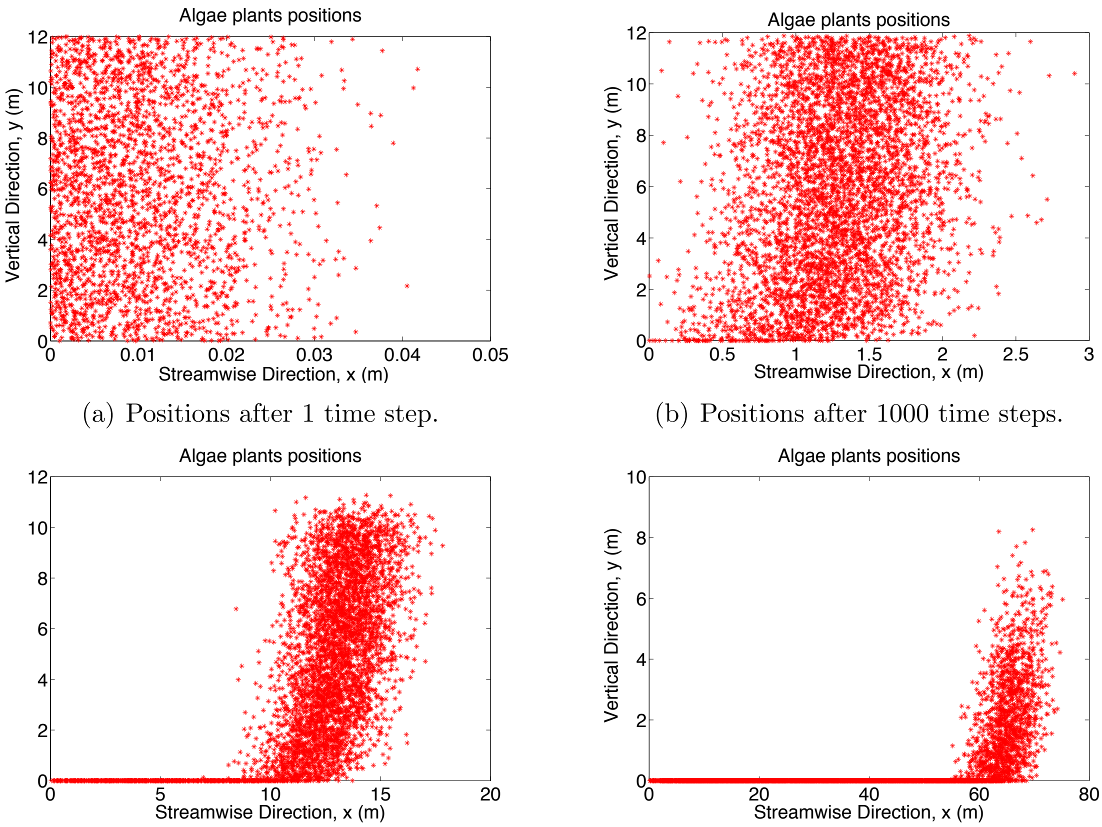

(a) Positions after 1 time step.

(b) Positions after 1000 time steps.

(c) Positions after 10000 time steps.

(d) Positions after 50000 time steps.

Figure 4.2: Positions of the algae plants for a logarithmic velocity profile in the smooth regime with varying diffusivity, including the noise induced drift component, the fall velocity and diffusion in the x-direction .

The concentration profile of the algae plants in the vertical direction is not affected as expected and also the average number of particles that will accumulate on the bed is also not affected by the diffusive step in the streamwise direction. This is shown by figure 4.3 which compares the vertical concentration profiles after 10000 timesteps with and without the inclusion of the diffusive step in the streamwise direction.

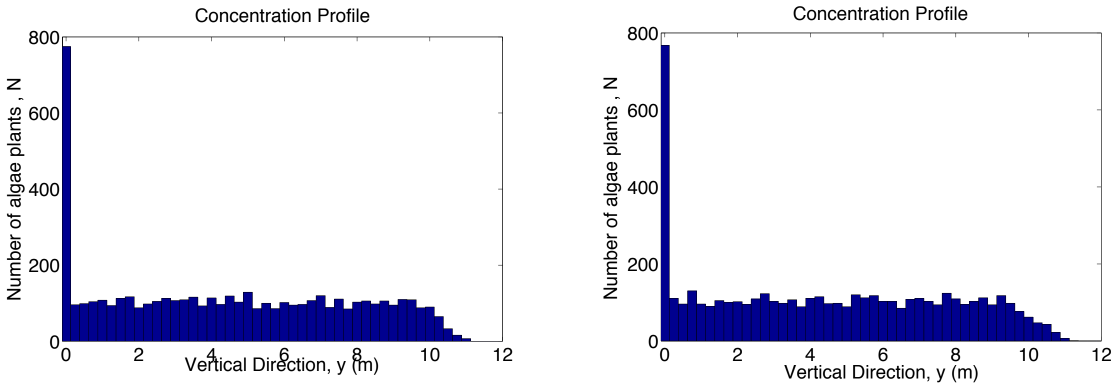

(a) Positions after 10000 time steps without diffusion in x-direction.

(b) Positions after 10000 time steps with diffusion in x-direction.

Figure 4.3: Concentration profiles of algae plants in the vertical direction with and without including the diffusive term in the streamwise direction.

From all the results presented and discussed in this chapter it is deduced that the inclusion of the random step in the streamwise direction, which represents turbulent diffusion, causes a stronger mixing of the algae plants in the corresponding direction. This effect though is visible and strong in the near filed.

Chapter 5

Interaction with band screen filters

5.1 Screening of algae plants

The interaction of the algae plants with the band screen is now investigated using the model discussed in section 2.2.8. The parameters for the simulations made are given by table 5.1.

Table 5.1: Simulation Parameters for the interaction with the band screen

Parameter	Value
Number of algae plants	5000
Diffusion coefficient, $D(y)$ (m^2/sec)	$\kappa u_* y(1 - y/h)$
Depth of channel, h (m)	12
Timestep, Δt (sec)	0.01
Drift component, $dD(y)/dy$	$\kappa u_*(1 - 2y/h)$
Fall velocity, w (m/sec)	0.0173
Velocity profile, $\bar{u}(y)$ (m/sec)	Eq. 2.2.1

In particular the algae plants are instantly released at the start of the intake filtration channel ($x = 0$), where they are uniformly distributed along the whole depth of the channel. The plants are advected in the streamwise direction and diffused in the vertical direction and will interact with the band screen after travelling a distance of 15 m in the streamwise direction, where the band screen is located. The vertical displacements of all the algae plants are calculated once they reach the band screen and some of the plants will pass through the screen while others will attach on the screen as previously discussed. Two parameters were defined in the developed model, the passing length and the blocking length, l_p and l_b respectively. Three different simulations were made based on different values of these parameters. The effectiveness of the band screen in filtering the algae plants depends on their flexibility and hence on the parameters defined in the model. The simulations made produce the results of figures 5.1, 5.2 and 5.3 which show the number of algae plants able to pass through the band screen at each specified opening along the length of the band screen. The band screen has a length which is equal to the depth of the channel (i.e 12 m). The results obtained from each of the three simulations are tabulated and are shown below the figures.

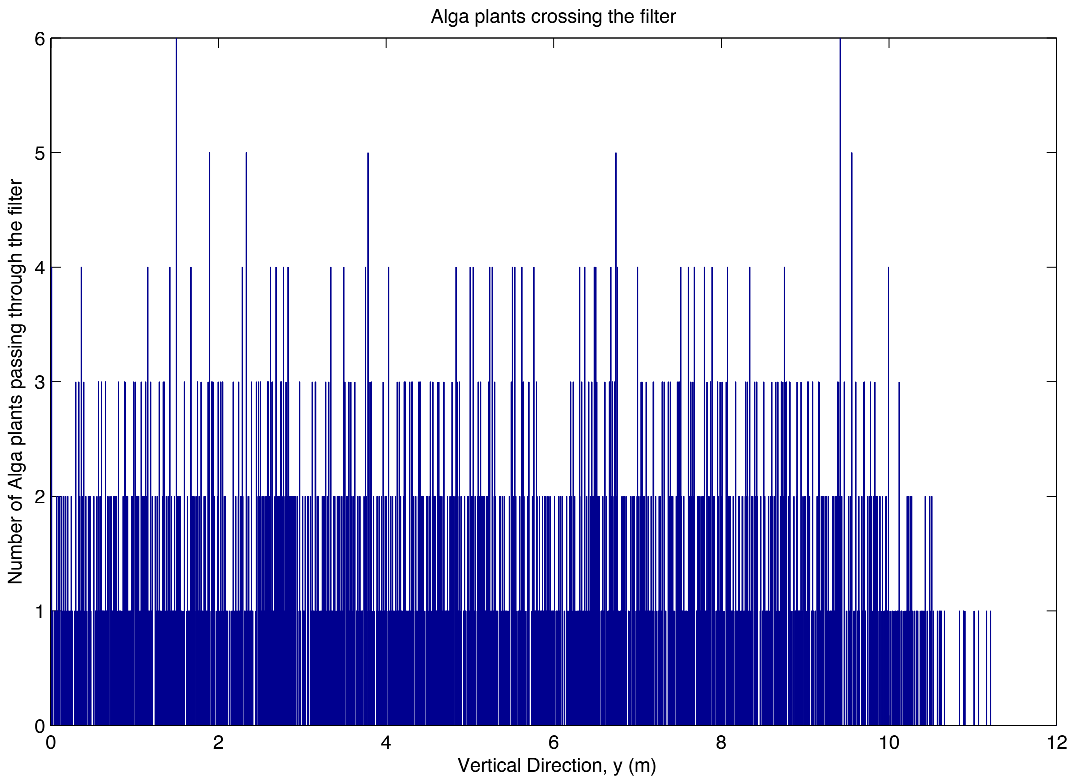

Figure 5.1: Distribution of number of algae plants passing through the band screen

Table 5.2: Simulation Parameters and Results

$l_b(mm)$	$l_p(mm)$	No. of plants passing	No. of plants blocked	No. of plants fallen on bed
3	3	2027	2017	956

Figure 5.1 shows the number of algae plants not filtered for $l_p = 3mm$ and $l_b = 3mm$. The maximum number of algae plants passing through a single opening is equal to 6, and this occurs in two cases. There is no indication however that this is related to the distance of the particular opening from the bed as the two cases mentioned occur at very different distances from the bed of the channel. Almost in all openings at least one alga plants is able to make it through the screen. Also the number of two algae plants passing through an opening is large. Note however that the mesh panels near the surface do not

contribute to the filtering of the algae plants. Three plants can make it through the band screen in approximately half of the openings. The numbers of four, five and six plants not filtered through the openings are small.

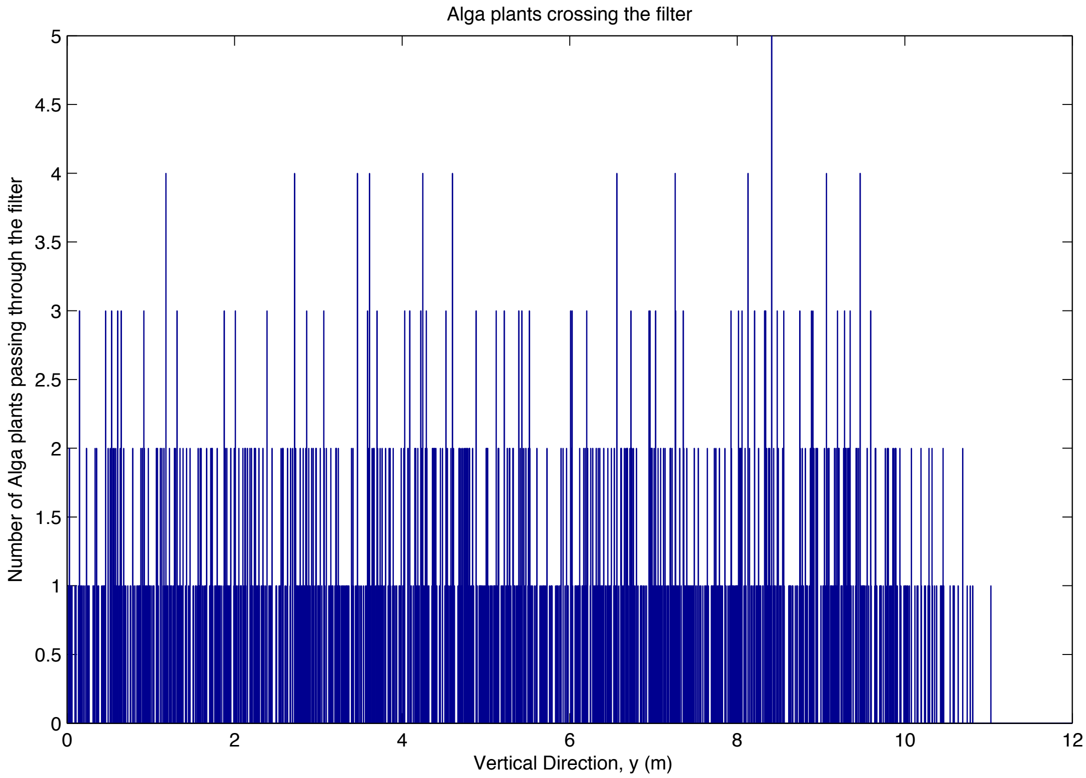

Figure 5.2: Distribution of number of algae plants passing through the band screen

Table 5.3: Simulation Parameters and Results

$l_b(mm)$	$l_p(mm)$	No. of plants passing	No. of plants blocked	No. of plants fallen on bed
4	2	1314	2750	936

Figure 5.2 shows the number of algae plants not filtered for $l_p = 2mm$ and $l_b = 4mm$. The maximum number of algae plants passing through a single opening now drops to five and occurs near the surface of the channel. Also in this case almost in all openings at least an alga plant is able to make it through the screen. Two plants are not filtered in approximately half of the openings. By comparing figures 5.1 and 5.2 we can see that the number of algae plants passing through each opening is reduced as expected. Again the mesh panels near the surface do not contribute to the filtration process.

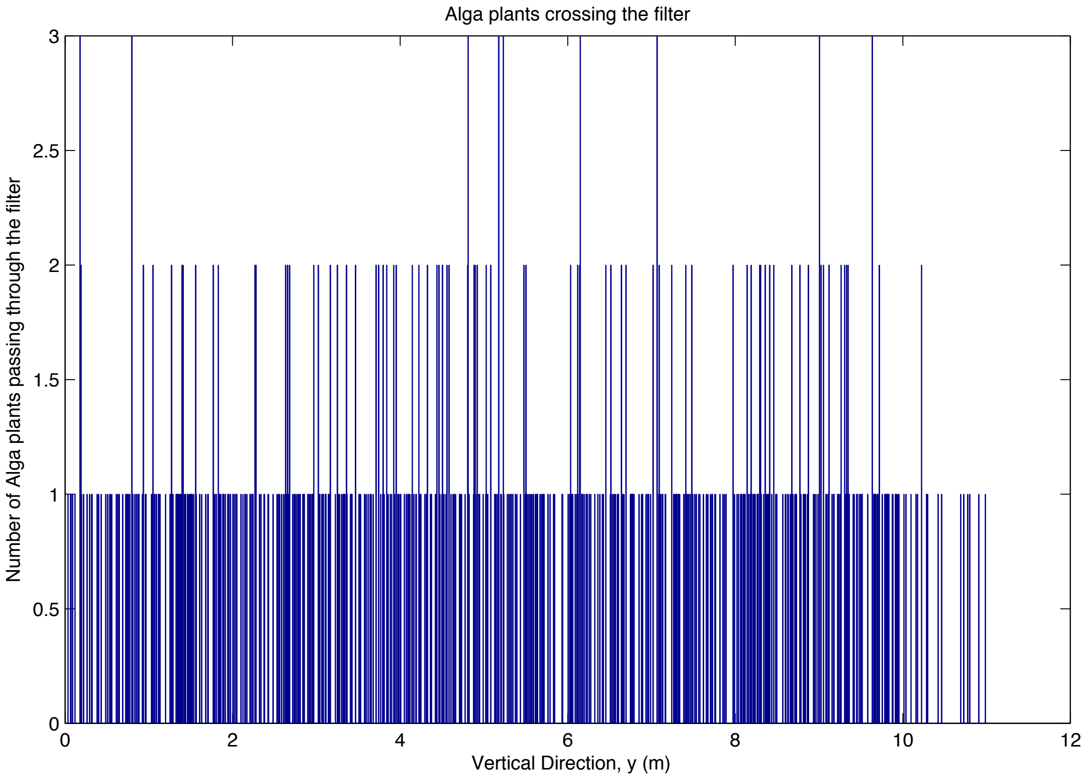

Figure 5.3: Distribution of number of algae plants passing through the band screen

Table 5.4: Simulation Parameters and Results

$l_b(mm)$	$l_p(mm)$	No. of plants passing	No. of plants blocked	No. of plants fallen on bed
5	1	640	3407	953

Figure 5.3 shows the number of algae plants not filtered for $l_p = 1mm$ and $l_b = 5mm$. The maximum number of algae plants passing through a single opening now drops to 3. Again in this case almost in all openings at least an algae plant is able to make it through the screen. By comparing this case to the previous cases we see that the number of algae plants passing through the screen has decreased significantly.

In all cases the model calculates very similar numbers of plants fallen to the bed which is approximately 20 percent of the total plants released. Further simulations with more particles were made that verify this observation. From the above results no indication could be derived about any preferred depth at which a plant is most likely to pass through the band screen.

The simulation suggest that the flexibility of a particular algae plant is an important parameter which determines the amount of plants filtered and hence the efficiency of a screen.

In reality it is expected that the complex with many fronds shape of the algae plants will make it even more difficult for a plant to pass through the screen as it will get tangled with the mesh. Furthermore when an algae plant is attached on the mesh then its fronds will have an effect on the blockage of nearby plants. These are the main limitations to the developed model.

5.2 Band screen blockage and Differential levels

In the previous section the flexibility of the algae plants was investigated and the effect this had on the interaction with the band screen. Algae plants that are not too flexible and have complex shapes will block the band screen and thus reduce the effective flow area through the screen. The reduction in the effective spacing of the mesh grid due to this blockage is now investigated. The head loss across the band screen is measured by a differential level control. This differential level determines the speed at which the band screens will start rotating and hence the cleaning process of the mesh panels starts. The table below shows the control actions of the band screen in relation to the differential level across it.

Table 5.5: Simulation Parameters

Differential level across band screen (mm)	Action
300	Low speed
400	High Speed
500	High Differential Alarm
575	Shut Down initiated
600	Maximum Design Differential

The low speed and high speed of the band screen are equal to 2.5 and 10 m/min respectively. Figure 5.4 shows the calculated differential levels across the band screen for different openings of the mesh grid as well as the levels where each action takes place. The analysis of obtaining these results follows below.
The Environmental protection agency gives in its waste-water treatment manual the head loss across a fine screen to be equal to:

$$\Delta h = \frac{1}{2gC}\left(\frac{Q}{A}\right)^2 \tag{5.2.1}$$

where Q is the maximum flow rate in m^3/sec, g is the acceleration of gravity (9.81 m/sec^2), A is the effective aperture area of the mesh in mm^2 and C is a coefficient given by the manufacturer [11] .
The total volumetric flow rate in the channel is equal to 27.5 m^3/sec. The flow passes through six band screens before entering the fore-bay from which the pumps draw the

filtered estuarine water. Hence the flow rate through each band screen is equal to 4.583 m^3/sec. The effective area of the mesh grid is chosen to vary depending on the effective opening (i.e the proportion of the aperture which in not blocked) . The coefficient C is given by the manufacturer to be approximately equal to one for the band screens investigated. By choosing different aperture openings the effective aperture area is calculated and the differential level across the band screen is then found using 5.2.1.

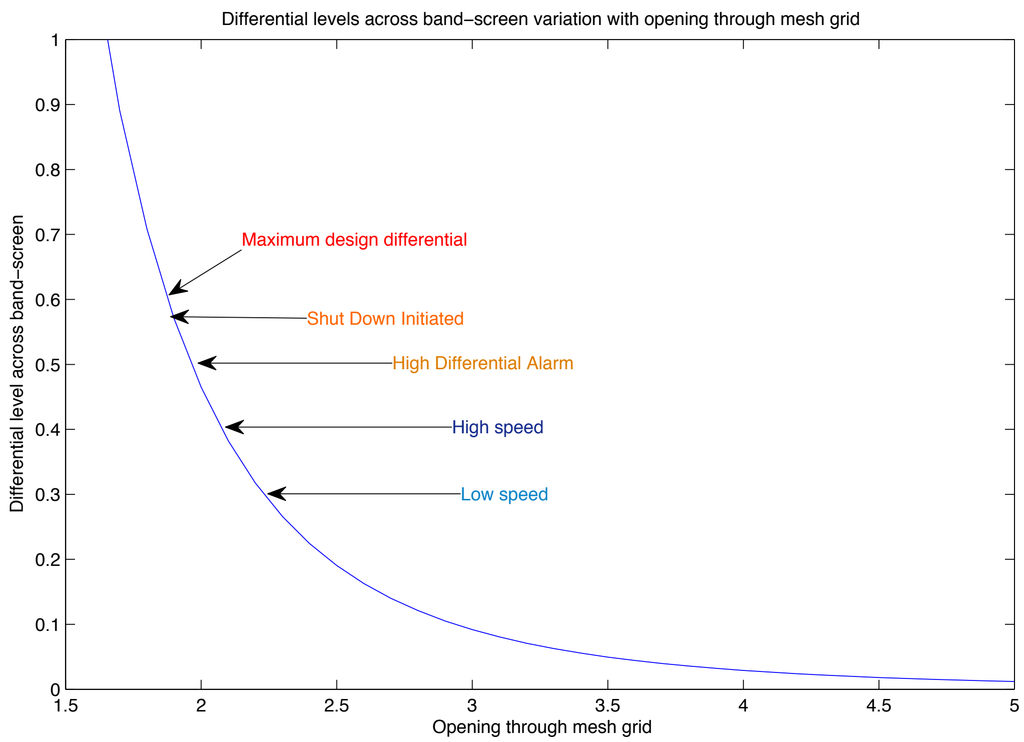

Figure 5.4: Variation of differential levels with opening of mesh grid

The effective openings can also be viewed as the percentage of the band screen that is clean and so water can pass through or considering the opposite approach how much of the band screen is blocked. The latter case is shown by figure 5.5. As the opening between the mesh grid is reduced the percentage of the band screen that is blocked increases.

The differential level across the band screen increases slowly for up to a blockage of around 70 percent and then increases sharply reaching a differential level equal to one near a 90 percent blockage. The actions taken for the control of the band screens lie between 80 to 86 percent blocked screen. When the mesh panels of the band screen are not adequately cleaned after a single passing through the cleaning system then a potential high differential alarm may be triggered as from the results we see that there is a high sensitivity between the differential levels, at which the actions take place, and the blocked percentage of the screen. A recalibration of the control of the differential levels of the actions is a potential solution to the problem initially presented. Doing so the sensitivity

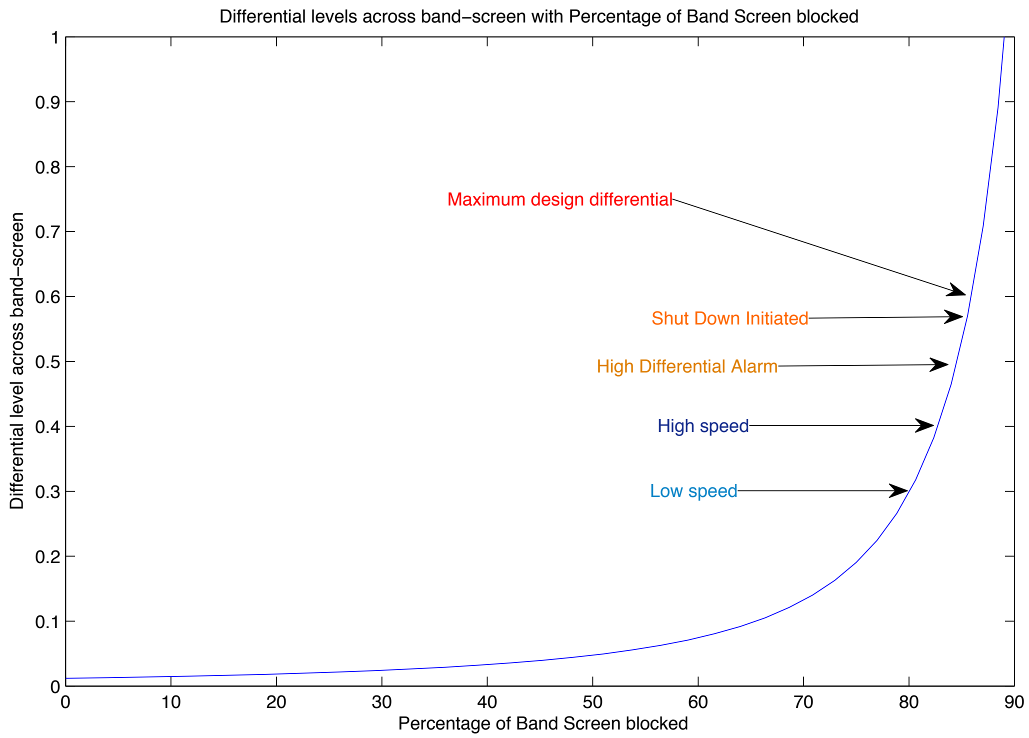

Figure 5.5: Variation of differential levels with percentage blockage of band screen

of the system will decrease thus reducing the possibility of triggering a high differential alarm or even damaging the band screens in the event of exceeding the maximum design differential.

Chapter 6

Conclusions and Further Work

6.1 Conclusions

The following conclusions were derived from the modelling of the algae trajectories in the intake filtration channel of South Humber Bank power station and their interaction with the band screens. The particle tracking method provides reasonable results for modelling the trajectories of the algae plants. A correction needs to be added to the governing equations in order to avoid the effect of particles gathering in low diffusivity regions.

The continuous release of the algae plants from the bed of the channel showed that the model describes the physical process of entrainment well.

The model developed is flexible as a different velocity profile can be implanted on the model and be used for other channel geometries.

The flexibility of an algae plant is an important parameter which affects not only the efficiency of filtration of the band screen but also the percentage of blockage of the band screen.

The inclusion of the fall velocity due to the buoyancy forces on the algae plants caused approximately twenty percent of the algae plants to accumulate on the bed before interacting with the band screen filters.

The diffusive step in the streamwise direction has a strong effect in mixing the algae plants, in the corresponding direction, in the near filed.

The mesh panels of the band screens near the surface of the channel (up to about 2 m below the water surface) do not contribute to the filtration process.

The differential levels of the controls, at which each action takes place, lie very close to eachother and are very sensitive to the blocked percentage of the band screen which, this may cause a high differential alarm to be triggered if the mesh panels are not adequately cleaned or damage the band screen if the maximum design differential is exceeded.

6.2 Further work

The model developed can be further improved by considering factors such as its accuracy and stability. Different schemes exist for developing efficient numerical methods for stochastic differential equations. The scheme used here was based on Ito, due to the relevant correction made. Other schemes include the Milstein scheme or Runge-Kutta methods. These methods provide greater accuracy but increase the computational needs. Field measurements may be recorded in order to compare these with the developed model and confirm the presented methodological approach. The actual velocity profile in the intake filtration channel can be found by suitable measurements on site, this can then be imposed in the developed model.

Acknowledgements

Centrica SHB for providing funding, information and data about the South Humber Bank power station. These include the travel expenses for the visit to the site, the work permit application of the station, the maintenance manual and drawings of the intake filtration channel. The writer would like to thank his project supervisor Dr. Liang D. for his guidance, help and advice throughout the duration of this project.

Bibliography

[1] Maintenance Manger Report . *Cooling Water cleaning system failure* 30^{th} *of December 2009* . South Humber Bank Power Station maintenance reports.

[2] I. Kaczmarska, L.L. Dowe . *Reproductive biology of the red alga Polysiphonia Lanosa (Ceramiales) in the bay of Fundy, Canada* . (1997) . Marine Biology 128: 695-703.

[3] Salamon P., Garcia D.F., Hernadez G.J. . *A review and numerical assessment of the random walk particle tracking method*. (2006). Journal of Contaminant Hydrology.

[4] Hathhorn E. W. . *Simplified approach to particle tracking methods for contaminant transport*. (1997) . Journal of Hydraulic Engineering.

[5] Kitanidis K. P. . *Particle tracking equations for the solution of the advection-diffusion equation with variable coefficients*. (1994) . American Geophysical Union.

[6] Weitbrecht V., Uijttewaal W. and Jirka G. H. . *2-D Particle Tracking to Determine Transport Characteristics in Rivers with Dead Zones*. (2003) . International Symposium on Shallow Flows.

[7] Ulf G. . *Implementation of high order particle tracking schemes in a water column model*. (2010) . Physical Oceanography and Instrumentation, Leibniz Institute for Baltic Sea Reasearch, Germany.

[8] Byron R.B., Warren E.S., Edwin N.L. . *Transport Phenomena*. (Second Edition 2007). John Wiley and Sons.

[9] R.A. Fralick , A.C. Mathieson . *Physiological Ecology of Four Polysiphonia Species (Rhodophyta, Ceramiales)* . (1975) . Marine Biology 29, 29-36.

[10] Liang D., Liang C., Li F. . *Numerical modelling and scour below a pipeline in currents Part II. Scour simulation.* (2005) . Coastal Engineering 52, 43-62.

[11] *Wastewater Treatment Manuals Preliminary Treatment.* (1995) . Environmental Protection Agency.

[12] Weiming Wu, Wolfgang R., Wenka T. . *3D Numerical modelling of flow and sediment transport in open channels.* (2000) . Journal of Hydraulic Engineering.

[13] Weitbrecht V., Kuhn, G.H. Jirka . *Large scale piv-measurements at the surface of shallow water flows.* (2003) . Flow measurements and Instrumentation 13(5-6) 237-245.

[14] Weitbrecht V., G.H. Jirka . *Flow patterns and exchange processes in dead zones of rivers* . (2001) . XXIX IAHR Congress, Beijing, China.

[15] Wong K.T.M., Lee J.H.W . *Simulation of harmful algal blooms using a deterministic Lagrangian particle separation-based method* . (2007) . Journal of Hydro-environment research.

[16] Zimmermann S. , Koumoutsakos P. , Kinzelbach W. . *Simulation of pollutant transport using a particle method.* (2000) . Journal of Computational Physics.

[17] James S.C., Chrysikopoulos C.V. . *An efficient particle tracking equation with specified spatial step for the solution of the diffusion equation.* (2001) . Chemical Engineering Science 56 6335-6543.

[18] RSK ENSR Group . *South Humber Bank Power Station PPC Permit Application* . (2006) .

[19] ABB Group . *South Humber Bank Power Station Maintenance manual* . (1988) .

Appendix A

A.1 Continuity

The volumetric flow rate drawn in from the Humber Estuary is 27.5 m^3/sec and area of the intake channel is 183 m^2 . Considering the continuity equation:

$$(\rho Q)_{pipe} = (\rho AU)_{channel} \Rightarrow U_{channel} = \frac{27.5m^3/s}{183m^2} = \mathbf{0.150}\ m/sec$$

A.2 Risk Assessment

Different risks and hazards were identified for this project. In this particular project a computer was used and the requirements of the workstation were a desk, chair and an electrical supply. The main hazards and their associated risks are:

1. An ergonomic issue developed from the wrong adjustment of the height of the desk and the chair used while working with the computer. This caused physical fatigue and pain in the back.
2.Low light conditions and the brightness of the screen were adjusted accordingly in order to avoid problems such as headaches and eye issues.
3. Noise was not an issue as in general a computer does not make too much noise and cannot affect a person's hearing.
4. Electricity from a faulty power supply is a potential hazard as it may hurt a person or damage the equipment used. Sockets were inspected before they were used.

In general due to the wide use of a computer as a tool for someone's work, most of the hazards and risks mentioned above were identified before the start of the project and relevant measures were taken.